

**HIGHER DIMENSIONAL COSMOLOGY:  
THE COSMOLOGY OF THE DGP MODEL**

**NG KAH FEE**

(B. Sc (Hons.) NUS)

**A THESIS SUBMITTED FOR THE DEGREE OF MASTER OF SCIENCE**

**DEPARTMENT OF PHYSICS**

**NATIONAL UNIVERSITY OF SINGAPORE**

**2013**

## Declaration

I hereby declare that this thesis is my original work and it has been written by me in its entirety. I have duly acknowledged all the sources of information which have been used in the thesis.

This thesis has also not been submitted for any degree in any university previously.



Ng Kah Fee

2 August 2013

## Acknowledgment

I have to thank Dr. Cindy Ng, my project supervisor. This project has been long and sometimes it can be taxing with all the tedious calculation and computation. Dr. Ng has been patient with me and has provided me with many fruitful discussions and guidance along the way.

I would like to also thank the examiners for pointing out the mistakes in the thesis. Their suggestions are much appreciated.

## Contents

<b>1</b>	<b>Introduction</b>	<b>1</b>
<b>2</b>	<b>Einstein's Equations and DGP Model</b>	<b>8</b>
2.1	Hilbert-Einstein Action . . . . .	8
2.2	DGP Model . . . . .	10
2.3	Metric . . . . .	12
2.4	Einstein's Equations . . . . .	13
2.5	Energy-Momentum Tensor . . . . .	14
2.6	Scalar Curvature Source Term $\tilde{U}$ . . . . .	15
2.7	First Integral of Einstein's Equations in the Bulk . . . . .	17
<b>3</b>	<b>Friedmann Equations and the Cosmology of DGP Model</b>	<b>20</b>
3.1	Friedmann Equations . . . . .	20
3.2	Junction Conditions for DGP Model . . . . .	22
3.3	5D Cosmology . . . . .	24
3.4	Recovery of Standard Cosmology . . . . .	25
3.5	Late-time Cosmology . . . . .	25
3.6	Cosmology of Phantom Energy Dominated Universe . . . . .	29
3.7	Brane Embedding in Minkowski Space-time . . . . .	29
<b>4</b>	<b>Cosmological Solution</b>	<b>34</b>
4.1	Cosmological Solution . . . . .	34
4.2	Luminosity Distance and Angular Diameter Distance . . . . .	37

4.3	Deceleration Parameter . . . . .	41
4.4	Effective Equation of State . . . . .	42
<b>5</b>	<b>Fitting of Parameters</b>	<b>46</b>
5.1	Minimum $\chi^2$ Test and Analytic Marginalization . . . . .	46
5.2	Normalization Condition . . . . .	53
5.3	Fitting Results: DGP Model with No Cosmological Constant . . . . .	56
5.4	Fitting Results: DGP Model with Brane and Bulk Cosmological Constants	57
<b>6</b>	<b>Future Investigation</b>	<b>65</b>
6.1	Schwarzschild Solution . . . . .	65
6.2	Schwarzschild Solution Again . . . . .	69
6.3	Diluting Cosmological Constant . . . . .	72
<b>7</b>	<b>Conclusion</b>	<b>74</b>

## Abstract

In recent years, observations suggest that our universe is expanding in an accelerating manner. There are two general directions in proposing models to explain the cosmic acceleration: one is to propose a valid cosmological constant or dark energy, the other is to propose a modified gravity theory. In the year 2000, Dvali, Gabadadze and Porrati, in the direction of modifying gravity, came up with an interesting model that uses extra dimensions.

The idea of higher dimensional cosmology is to propose a model with more than 4 dimensions such that the extra dimensions remain undetectable in the normal scale range, yet they will manifest themselves in certain ways that will provide the acceleration required. The model proposed by Dvali, Gabadadze and Porrati (DGP model) is set in a 5D bulk consisting of 4 spatial dimensions and 1 temporal dimension. In this model, all the matter and energy contents are confined to a 3D brane and the action governing the gravitational interaction is the normal 5D Hilbert-Einstein action with an extra 4D Hilbert-Einstein term. This extra 4D action will ensure that on smaller scales, like the scale of the solar system, the action will act like the 4D Hilbert-Einstein action of 4D General Relativity, so that the extra spatial dimension will pass the solar system tests without being detected. On the other hand, on larger scales, the action will be dominated by the 5D term, so that the model will act like a true 5D model which expands faster than a 4D model, providing the acceleration required.

In this thesis, we follow the DGP model and rederive the equation of motion. Using the Friedmann equation, we examine the cosmology of this model and subject it to some observational tests. We also briefly introduce some unexplored aspects of the model. Finally, we give a conclusion and reiterate the results of the fitting.

## List of Tables

1	The best-fit of three different methods of marginalization of $h$ . . . . .	49
2	The best-fits of marginalization over $h$ , $M$ , or both. . . . .	53
3	The fitting result of <i>Brane 2</i> using Riess and SNLS data with no cosmological constant. . . . .	58
4	The fitting result of a flat <i>Brane 2</i> with no cosmological constant: $\Omega_k = \Omega_\Lambda = \Omega_B = 0$ . . . . .	58
5	$\chi^2$ of a flat <i>Brane 2</i> with $\Omega_M = 0.3$ and no cosmological constant: $\Omega_k = \Omega_\Lambda = \Omega_B = 0$ . . . . .	58
6	The fitting result of the $\Lambda$ CDM model, i.e. $\Omega_{r_c} = 0$ . . . . .	58
7	$\chi^2$ of the $\Lambda$ CDM model, i.e. $\Omega_{r_c} = 0$ , with $\Omega_M = 0.3$ . . . . .	58
8	Best-fit of <i>Brane 1</i> and <i>Brane 2</i> assuming a flat universe. . . . .	58
9	Best-fit of <i>Brane 1</i> and <i>Brane 2</i> assuming a flat universe with $\Omega_M = 0.3$ . . .	62
10	Best-fit of <i>Brane 1</i> and <i>Brane 2</i> assuming a flat universe with only the brane constant. . . . .	62
11	Best-fit of <i>Brane 1</i> and <i>Brane 2</i> assuming a flat universe with only the brane constant and $\Omega_M = 0.3$ . . . . .	62
12	Best-fit of <i>Brane 2</i> assuming a flat universe with only the bulk constant. . .	62
13	Best-fit of <i>Brane 2</i> assuming a flat universe with only the bulk constant and $\Omega_M = 0.3$ . . . . .	62

## List of Illustrations and Figures

1	An artistic illustration of the space-time fabric being bent by masses such as planets in the universe. . . . .	9
2	Luminosity distance of different models. . . . .	40
3	Angular diameter distance of different models. . . . .	41
4	Deceleration parameter, $q$ of various models. . . . .	43
5	Time-dependent $\Omega_M$ of various models. . . . .	44
6	Contours of $\chi^2$ of different marginalization techniques. . . . .	50
7	The fitting result of SN1a (Riess 2004) with the prior from BAO (Eisenstein 2005). . . . .	51
8	The fitting results of SNLS data with different marginalizations. . . . .	54
9	The SNLS data fitted using type 3 analytic marginalization with a prior from BAO. . . . .	55
10	<i>Brane 1</i> and <i>Brane 2</i> with brane and bulk constant, $\Omega_M = 0.3$ . . . . .	60
11	<i>Brane 1</i> and <i>Brane 2</i> with only brane constant. . . . .	63
12	The plot of luminosity distance using the best-fit of Table 9. . . . .	64



## 1 Introduction

The universe is a mysterious place, and humans from all ages have been drawn to it for different reasons. Even in this modern age of science and technology, when mankind has learned to fly and explore the earth's atmosphere, the great universe beyond still remains relatively unexplored. For many years cosmologists and particle physicists have been trying to solve the mystery of our ever expanding and intriguing observable universe. In more recent years, the idea of an expanding observable universe has taken on a whole new meaning with the discovery that the universe is literally expanding in an alarming manner. From the observations made, most physicists agree that our universe is expanding in an accelerating manner, which raises the questions of why this is happening and what lies ahead. Many different theories and models have been proposed to explain this surprising yet exciting phenomenon, and, as with any other scientific theory, to make an accurate prediction of the future. Different physicists have different approaches when it comes to explaining new phenomena. The theorists try to propose a working effective theory of gravity based on more fundamental theories like the string theory and other quantum gravity candidates. Some cosmologists would work on model building by proposing different actions or adding ingredients, and they use ideas coming from particle physics, or some ad hoc ideas that fits the observations. Of all these proposed models, the most widely accepted one is without doubt the  $\Lambda$ CDM model.

The  $\Lambda$ CDM model is relatively simple compared with the other models. It assumes the simple Friedmann-Lemaître-Robertson-Walker metric:

$$ds^2 = -dt^2 + a^2(t) \left[ \frac{dr^2}{1 - kr^2} + r^2(d\theta^2 + \sin^2\theta d\phi^2) \right] \quad (1)$$

where  $(t, r, \theta, \phi)$  is the usual temporal and 3 spatial comoving coordinates,  $a(t)$  is the scale factor and  $k = -1, 0, 1$  corresponds to open, flat and closed universes respectively. The idea of proposing said metric comes from the assumption of a homogeneous and isotropic universe which is reflected in the total symmetry of the spatial coordinates, and the scale factor is added to show the homogeneous and isotropic expansion of the universe. The acronym  $\Lambda$ CDM represents the two main components of our universe in this model: the cosmological constant  $\Lambda$  and the matter (the normal baryons and the cold dark matter) [1]. From a broader perspective, the cosmological constant term can be classified as a source of dark energy, which sounds similar to the notion of dark matter, but is a completely different idea. The term cold dark matter is used to reflect the idea that it does not emit

any radiation, but it is in fact a matter term and it interacts gravitationally just like any normal baryon. On the other hand, the dark energy term interacts differently in terms of gravitation; it is a bizarre source of energy that has a negative pressure, which can be used to counteract the attraction between the matter sources. The idea of cosmological constant first came from Einstein himself, after he established the well-known General Relativity. He first proposed this idea of adding a constant to the Einstein equations to reach a static solution for the universe, but he soon abandoned the idea when the expansion of the universe was discovered. Many years later, the discovery of the acceleration of the expansion was made, and physicists were challenged again to find a model of our universe that expands in an accelerating manner, at least at the current epoch. Under such circumstances, the cosmological constant made a return with the proposal of the  $\Lambda$ CDM model. In this simple yet elegant model, the universe is governed by the Friedmann equations [1]:

$$\begin{aligned} H^2 \equiv \left(\frac{\dot{a}}{a}\right)^2 &= \frac{8\pi G}{3}(\rho + \varepsilon) - \frac{k}{a^2} \\ \frac{\ddot{a}}{a} &= -\frac{4\pi G}{3}(p + 3\rho + 2\varepsilon) \end{aligned} \tag{2}$$

where  $\rho$  and  $\varepsilon$  are the energy densities of matter and the cosmological constant respectively. Note that the equation is the same as the counterparts in other General Relativity models, except that we only have 2 components for the energy density, and the cosmological constant has an equation of state of  $w = p/\rho = -1$ . With this set of equations, we can derive the whole cosmology of the model, which closely fits most current observations. This is a clean and simple model, but many theorists believe that the model is incomplete because of a well-known problem concerning the origin of the cosmological constant, which is commonly known as the cosmological constant problem. Many theorists believe that the cosmological constant originates from the vacuum energy in particle physics, but the value proposed by the theory is too large and will cause the expansion to accelerate at a much faster pace than the observation. The difference between this theoretical value and the measured value is so large ( $\sim 10^{130}$  order of magnitude) that fine-tuning the model to cancel the effect of cosmological constant seems highly unnatural. Until the cosmological constant problem is resolved, the  $\Lambda$ CDM model can never be accepted as the whole truth.

As in many historical examples of disagreement between a well-established theory and the experiments, there are currently two major directions that attempt to solve the cosmological constant problem. A good example to illustrate these two different directions is the two disputes of planetary trajectory in our own solar system in the 19th century. The first case is the disagreement between the trajectory of Uranus and the prediction of classical

Newtonian mechanics, and it eventually led to the discovery of Neptune by Le Verrier. When Le Verrier and others tried to apply the same method to solve the problem of Mercury's perihelion precession, it did not work. It turned out that this abnormal phenomenon could only be explained by a modification of Newtonian gravity by General Relativity, and Mercury's perihelion precession has since become one of the major tests for all modified gravitational theories. In summary the first case shows the triumph of adding a new ingredient to the model, which is the new planet Neptune; in the second case, it was discovered that the theory is incomplete. In our situation of the cosmological constant problem, the first case would correspond to the cosmologists trying to change the components of the universe. They replace the cosmological constant that causes the problem. Some cosmologists are searching for a new type of energy density, and the common consensus among them is to search for scalar fields that vary over the course of time. With a slowly changing field, it is hoped that we can avoid the fine-tuning problem and have a theoretically acceptable value for the dark energy. On the other hand, the second direction attempting to solve the problem is to modify the theory of General Relativity and replace it with a more general theory. Ideally, this new theory would behave like General Relativity on smaller scales and would only manifest itself on the scale of cosmological distances. Up to date, searches for a convincing dark energy model and a well-established modified gravity theory are both equally probable in solving the problem. In the year 2000, Dvali, Gabadadze and Porrati, in the direction of modifying gravity, came up with an interesting model that uses extra dimensions to solve this dilemma [2]. This is the topic that I would like to discuss in length in my thesis.

As we all know, after Einstein proposed his theory of Special Relativity and later the theory of General Relativity, people now commonly accept that our world is composed of not 3, but 4 dimensions: 3 spatial dimensions and a temporal dimension which is time. With improved precision of measurements, the old Newtonian mechanic is challenged with puzzling disagreements with the observation. A good example of such problem is when one tries to locate oneself using moving satellites orbiting tens of thousands of kilometers away from earth, Newtonian prediction is too far off to be of any use. In other words, the Global Positioning System (GPS) is not possible without the General Relativity correction. This leap from the 3 dimensions in Newtonian gravity to the 4 dimensions in General Relativity has solved many such problems. More importantly, the new theory also predicts various new phenomena like the gravitational lensing which are subsequently verified in cosmological observations. The idea of adding dimensions to our world seems shocking at first, but Einstein has shown that it is plausible with his theory of General Relativity. As it turns

out, the framework of General Relativity is not limited to 4D, it can be easily extended to more dimensions. This gives us a new direction in exploring the laws of physics and since then, many other physicists have ventured into the higher dimensional physics, notably the higher dimensional cosmology.

The idea of higher dimensional cosmology is to propose a model with more than 4 dimensions that can help to solve some remaining mysteries of the universe, in particular the cosmic acceleration. The idea of extra spatial dimensions first came from Kaluza and Klein over 80 years ago [3]. The Kaluza and Klein theory is mainly an extension of General Relativity to 5D with some extra conditions to justify the invisibility of the 5th dimension to us. The first condition, also known as the ‘cylinder’ condition, was proposed by Kaluza and it consists of setting all partial derivatives with respect to the 5th dimension to zero. This is a very strong constraint, but thanks to it, the algebraic part of the theory can be reduced to a more manageable level. The other constraint in the model is the compactification constraint proposed by Klein, which specifies that the extra dimensions are not only finite and very small in length, but also have a closed topology. For example, in the most common case when we only have one extra dimension, the 5th dimension will be a circle. In this theory, there is an induced-matter discussion in which our usual 4D matter can be regarded as induced from an empty 5D space. More precisely, in the case of an empty universe, we have the usual Einstein’s equation  $G_{AB} = 0$ , or equivalently,  $R_{AB} = 0$ . If we focus on the 4D part of the tensor equation and regard all the terms involving the 5th dimension as a source term, and put them on the other side of the equation, we will have our induced-matter equation:

$$G_{\mu\nu} = \rho(b, \dot{b}, b', \dots) \quad (3)$$

where  $b$  is the coefficient of the 5th dimension of the metric  $g_{AB} = g_{\mu\nu} + b^2(\tau, y)dy^2$  and  $\dot{b}$  and  $b'$  denote derivatives with respect to time and the 5th dimension,  $y$ , respectively. In other words, our 4D universe with certain matter density distribution is equivalent to a 5D empty universe with appropriate parameters. Since then, even though the Kaluza-Klein theory itself has some problems that render the model unsuccessful, the topic sparked an interest in understanding 5D universes of different types, and later models with even higher dimensions, notably the 10D braneworld models from string theory. There are different theories as to where the extra dimensions come from, but the theories mostly support extra spatial dimensions. Here, we are only interested in adding one extra spatial dimension, so we turn to the DGP model which is one of the most widely studied 5D cases.

There are a few ways to construct a 5D version of our world. At first glance, adding an

extra dimension is just adding an extra entry to our usual column vector and some might think that this is not much of a change, but they cannot be more wrong. As most people who dabble in vector calculus know, a lot of the theories of vector spaces depend on the dimensionality and after adding extra dimensions, we have fundamentally changed the laws of physics. In cosmology, the most fundamental force that we deal with is the gravity. A 5D gravity is generally weaker than a 4D gravity, and their main difference is that the former decays at a rate of  $1/r^3$  while the latter decays at a rate of  $1/r^2$ . To grasp the idea that gravity is generally weaker in higher dimensions, we can consider a Newtonian mechanics analogue. Assuming Newton's law of gravity holds both in 3D and 4D, and the attractive potential is given by the mass, or equivalently, the density:

$$\text{div}(\vec{g}) \propto \rho \quad (4)$$

Then the gravitational potential  $g$  can be calculated from the mass in question:

$$M = \int \rho dV \propto \int \text{div}(\vec{g}) dV = \oint \vec{g} \cdot d\vec{S} \quad (5)$$

Assuming an isotropic case like in the case of a point mass, then the magnitude of the gravitational potential  $g$  is the same in every direction. If we integrate over a sphere centered around the point mass in the 3D case, the total surface area  $\oint dS$  is simply  $4\pi r^2$ , so we have the usual relation:

$$\begin{aligned} M &\propto g \cdot 4\pi r^2 \\ g &\propto M/r^2 \end{aligned} \quad (6)$$

We have then recovered the inverse square law of gravity where  $g$  decays at a rate of  $1/r^2$ . On the other hand, in the 4D case the total surface area is given by  $2\pi^2 r^3$ , so we have

$$\begin{aligned} M &\propto g \cdot 2\pi^2 r^3 \\ g &\propto M/r^3 \end{aligned} \quad (7)$$

We can see that  $g$  decays at a rate of  $1/r^3$  as mentioned earlier.

From the simple analogy above, we see clearly that gravity behaves differently in 3D and in 4D, and we can imagine that the 4D and 5D gravities will also be very different. Hence to have an acceptable 5D gravity, there must be an effective mechanism to make the proposed 5D gravity behave like a 4D one in our daily observations. One way for the 5D gravity to avoid detection is to make the extra dimension very small, like in the case of the Kaluza-Klein model, or warped, like in the case of the Randall-Sundrum model (RS)

proposed by L. Randall and R. Sundrum [4]. In these models, because of the small length of the extra dimension, the 5D gravity behaves like a normal 4D gravity in macroscopic observations like the planetary interactions, and only under the fine scrutiny of very small scale we can hope to find signs of the actual 5D gravity. The RS model is one of the working models with small extra dimensions, and there are other ways to hide the 5D gravity from normal detections. On the other end of the spectrum, one plausible solution is to make the extra dimension very large.

Contrary to the common belief that extra dimensions can only exist in very small lengths, Dvali, Gabadadze and Porrati proposed a working model with a large extra dimension. In this DGP model, the extra spatial dimension is infinite in length and it is assumed that we live in a 3-dimensional static brane that is embedded in the 5D bulk. The idea of a braneworld where all matter or energy densities are restricted to a 3D brane is quite common, and almost all models originated from string theory, like the RS model mentioned previously, use the braneworld structure. With the success of such models, other cosmologists also came up with different braneworld models which are not entirely based on the string theory. They use many different and more ad hoc actions in the models, trying to construct an action that resembles the 4D gravity on smaller scales like the scale of the solar system, and yet solves the cosmological constant problem on larger scales. In the DGP model, instead of using the usual 5D Hilbert-Einstein action like in the case of General Relativity, we use an action that includes an additional 4D Hilbert-Einstein action:

$$S_{(5)} = -\frac{1}{2\kappa^2} \int d^5X \sqrt{-\tilde{g}} \tilde{R} + \int d^5X \sqrt{-\tilde{g}} L_m - \frac{1}{2\mu^2} \int d^4X \sqrt{-g} R \quad (8)$$

With this extra 4D action, the gravity will appear to be 4D on small scales, but will slowly decay into 5D gravity on larger scales. Since the 5D gravity is weaker than the 4D one, the expansion of the universe on a larger scale will be faster because of a weaker attractive force. In fact, we will see later in Section 3 that in the DGP model, one can achieve the cosmic acceleration without a cosmological constant. In that case, no fine-tuning will be needed and the cosmological constant problem can be avoided.

In this thesis, we follow exclusively the DGP model as mentioned. In Section 2, we dabble into the cosmology of higher dimensions. We rederive the Einstein's equations in a 5D braneworld setting as in the DGP model, but we see that the equations are also applicable to a more general set of braneworlds. Then in Section 3, we rederive a modified Friedmann equation which is more specific to our model. With that, we can discuss qualitatively some cosmological aspects of the DGP model such as the recovery of the standard cosmology and

the prediction for late-time cosmology. In that section, we see for the first time that there are two branches of solutions to the DGP model and one of them, which we call the *Brane 1* solution, shows a close resemblance to the phantom energy model. The phantom energy is one of the more exotic dark energies. This form of energy has an equation of state of  $w < -1$ , so it violates the energy conservation principle by increasing indefinitely with time, and hence is not taken seriously by most cosmologists. Contrary to the phantom energy model, the *Brane 1* solution has a similar evolution but does not violate the conservation of energy. At the end of that section, we also discuss briefly how the embedding of a 3D brane in the bulk can be done smoothly without causing singularities in the metric.

Subsequently in Section 4, we develop a proper cosmological solution to the model. We also discuss more in depth the phenomenology of the cosmology in terms of various observed quantities. After the qualitative discussions, we subject the DGP model to a maximum likelihood test to quantitatively compare the model with other models, including the  $\Lambda$ CDM model, in Section 5. There are different methods of implementing the minimum  $\chi^2$  test and they are discussed in details in this section. The result of fitting the parameters is given at the end of the section, followed by detailed discussions. Some on-going work on the DGP model and the attempts to generalize the model are introduced in Section 6. Lastly, in Section 7, we give a conclusion on this study of the DGP model.

## 2 Einstein's Equations and DGP Model

There are many different models of higher dimensional cosmology, and the number of extra dimensions can vary. As mentioned in the introduction, we will follow the setting of the DGP model [2] which assumes that we live in a 3D static brane that is embedded in a (4+1)-D universe. In this setting, the 5D bulk is comprised of 4 infinite spatial dimensions and 1 temporal dimension. The extra infinite dimension is the key ingredient that will separate this model from the conventional 4D model and the higher dimensional models with finite extra dimensions. In the discussions that follow, 0, 1, 2, 3 and 5 are used to denote the temporal coordinate, the three usual spatial coordinates and the extra spatial coordinate respectively, capital roman letters like  $A, B$  are used to denote indices running from 0 to 5, small greek letters like  $\mu, \nu$  are used to denote indices running from 0 to 3.

### 2.1 Hilbert-Einstein Action

Before we introduce the DGP model, it is beneficial that we review briefly the General Relativity from a field theory approach. In this theory, which was proposed by Albert Einstein in 1916, the traditional idea of a gravitational force between masses is replaced by the space-time fabric. Einstein extended the idea of space-time in Special Relativity and proposed that the trajectory of any object with a mass (or energy as we will see) is completely determined by the structure or the curvature of the space-time fabric. The role of mass surrounding the said object is to modify the space-time in its vicinity. This fabric of space-time that governs the trajectory of all objects is represented by a mathematical object called the metric. The metric of a physical coordinate system measures the distances and the structure of the coordinates, or in our case the space-time, so the metric has all the information required to determine the kinematic of any object in the system. More over, Einstein also proposed the equivalence of mass and energy in gravitational interactions, hence the famous equation  $E = mc^2$ . In other words, an energy source in the universe can bend the space-time as much as any ordinary matter. Putting all these ideas in the language of mathematics, the gravitational interaction between any masses or energies is governed by the following equations, known as Einstein's equations:

$$G_{\mu\nu} \equiv R_{\mu\nu} - \frac{1}{2}Rg_{\mu\nu} = 8\pi GT_{\mu\nu} \quad (9)$$



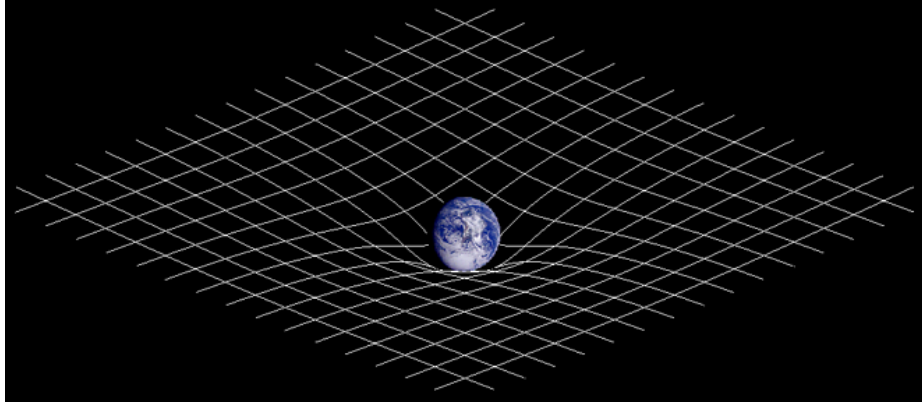


Figure 1: An artistic illustration of the space-time fabric being bent by masses such as planets in the universe. (Wikipedia, <http://en.wikipedia.org/wiki/Spacetime>)

On the right-hand-side of the equation, we have Newton's gravitational constant  $G$  and  $T_{\mu\nu}$  is the energy-momentum tensor. This is the term that encompasses all the energies or, equivalently, masses in the equation and it acts as the source term of the equation, much like the mass  $M$  acting as the source of gravitation in Newton's equation,  $g = GM/r^2$ . On the other side of the equation, we have terms that account for the structure of space-time including the Ricci tensor  $R_{\mu\nu}$ , the Ricci scalar  $R$  and the metric of the space-time  $g_{\mu\nu}$ , and all these terms are combined into a single tensor known as the Einstein tensor,  $G_{\mu\nu}$ . In short, this equation controls how the fabric of space-time is shaped by the energies and masses, and all energies and masses in the equation will move according to this space-time fabric. This is a real-time interactive equation as the masses involved in changing the space-time landscape are themselves bounded by the landscape and have to move accordingly. This makes it a very difficult differential equation to solve. Hence in cosmology and astrophysics, we often have to start with certain assumptions, notably the symmetries in the model, to simplify the equation and eventually solving it. We will see the use of symmetry in many occasions throughout this thesis.

Having seen the Einstein's equations which governs all interactions between masses, there are different approaches to understand the equation, one of which is the field theory approach. The field theory approach is not uncommon in the studies of fundamental physics. It originates from the Lagrangian method of studying the Newtonian mechanics and it can be applied to many different fields, most famously to quantum physics. In this approach, one has to find an action which governs the interaction between the objects. In our case, we have to find an action which can lead us back to the Einstein's equations, and that turns

out to be the Hilbert-Einstein action:

$$S = -\frac{1}{2\mu^2} \int d^4X \sqrt{-g} R + \int d^4X \sqrt{-g} L_m \quad (10)$$

where  $g$  is the trace of the metric,  $R$  is the Ricci scalar mentioned previously, and  $L_m$  is the matter lagrangian. In the field theory approach, the proposed action of the model always satisfies the least action principle. The principle dictates that one object will always follow the trajectory of least action to go from one place to another, i.e. the variation of the action  $\delta S$  should be 0 for any variation of the trajectory. If we vary the action (10), we get:

$$\delta S = -\frac{1}{2\mu^2} \int d^4X \sqrt{-g} (R_{\mu\nu} - \frac{1}{2} R g_{\mu\nu}) \delta g^{\mu\nu} + \int d^4X \frac{1}{2} \sqrt{-g} T_{\mu\nu} \delta g^{\mu\nu} \quad (11)$$

where the energy-momentum tensor  $T_{\mu\nu}$  is conveniently chosen to be:

$$T_{\mu\nu} = \frac{2}{\sqrt{-g}} \left[ \frac{\delta(\sqrt{-g} L_m)}{\delta g^{\mu\nu}} - \left( \frac{\delta(\sqrt{-g} L_m)}{\delta g'^{\mu\nu}_{,\alpha}} \right)_{,\alpha} \right] \quad (12)$$

If we combine the integrations in Equation (11), we have:

$$\delta S = \int d^4X \frac{1}{2} \sqrt{-g} \left[ -\frac{1}{\mu^2} (R_{\mu\nu} - \frac{1}{2} R g_{\mu\nu}) + T_{\mu\nu} \right] \delta g^{\mu\nu} \quad (13)$$

Since we have  $\delta S = 0$  for any  $\delta g^{\mu\nu}$ , we must have zero for the integrand:

$$\frac{1}{\mu^2} (R_{\mu\nu} - \frac{1}{2} R g_{\mu\nu}) = T_{\mu\nu} \quad (14)$$

By choosing the constant  $\mu$  such that  $\mu^2 = 8\pi G$ , we can recover the Einstein equation. In other words, choosing the action in a model will determine the interactions between the objects and hence the whole cosmology in our case.

## 2.2 DGP Model

Having seen the Hilbert-Einstein action, we can now define the action for the DGP model in the 5D bulk [5]:

$$S_{(5)} = -\frac{1}{2\kappa^2} \int d^5X \sqrt{-\tilde{g}} \tilde{R} - \frac{1}{2\mu^2} \int d^4X \sqrt{-g} R + \int d^5X \sqrt{-\tilde{g}} L_m \quad (15)$$

where  $\tilde{g}$  is the trace of the 5D metric,  $\tilde{R}$  is the 5D Ricci scalar, while the non-tilde terms  $g_{\mu\nu} = \partial_\mu X^A \partial_\nu X^B \tilde{g}_{AB}$  is the induced metric in the brane with trace  $g$ ,  $R$  is the corresponding Ricci scalar, and finally  $L_m$  is the matter lagrangian which represents the contribution of all the energy densities as usual. Note that in addition to the usual 5D Hilbert-Einstein action, we have added an extra 4D curvature term in the middle which is not a direct 5D generalization of the General Relativity, and this will be the key term responsible for maintaining a 4D Newtonian gravity on smaller scales. It is mentioned by Sahni and Shtanov [6] that it is possible to have a different sign for the 5D action, but as we will show later in Section 3, this difference in sign will not have any impact on the brane cosmology. It does not affect directly the fitting of the model to the observations, but it can have an effect on how the brane is embedded in the bulk, and thus may be important in the study of the perturbations of the theory.

As mentioned at the start of the section, all the usual matter we perceive are restricted in a 3D brane. In addition to a homogeneous bulk fluid, we also include a brane-localized matter term to account for our usual matter. The reason that all forces and particles are confined to the brane can be attributed to a filter of mass by the energy scale involved [7]. This filter applies for all interactions except gravity, which is free to permeate in all dimensions. To account for these contributions, we have the brane-localized term which is only 4-dimensional and takes the form of

$$\int d^4x \sqrt{-g} (\lambda_{brane} + l_m)$$

where  $\lambda_{brane}$  is the brane tension. As we can see in the action above, the brane tension has a similar role to a corresponding 4D cosmological constant, and hence forth we will mainly focus on the latter.

Another thing to note in the action is the coefficients of the integrations. They are related to the Newton's gravitational constant and planck mass of the corresponding dimension:

$$\begin{aligned} \kappa^2 &= 8\pi G_{(5)} = M_{(5)}^{-3} \\ \mu^2 &= 8\pi G_{(4)} = M_{(4)}^{-2} \end{aligned} \tag{16}$$

In our discussions, they are assumed to be independent of each other. It is mentioned by Deffayet [5] that in this setting, the 4D gravitational constant will be smaller than the conventional Newton's constant:

$$G_N = \frac{4}{3} \frac{\mu^2}{8\pi} = \frac{4}{3} G_{(4)}$$

This will have a non-negligible phenomenological effect on the cosmology, but it is still interesting to see how the intrinsic curvature term we added can play a similar role to that of a cosmological constant in the evolution of the universe.

Finally, to see the cosmological effects on different scales, we define a cross-over scale beyond which our usual 4D gravity will cross-over to a 5D gravity [2]:

$$r_c = \frac{M_{(4)}^2}{2M_{(5)}^3} = \frac{\kappa^2}{2\mu^2} \quad (17)$$

This cross-over scale will be referred to extensively in our discussions on the phenomenology of the DGP universe.

### 2.3 Metric

In cosmology, the metric of a model is a fundamental quantity that will indirectly change the cosmology. The kinematic is governed directly by the metric which in turn is controlled by the energy distribution via Einstein's equations. In General Relativity, the most commonly accepted metric for our universe is the Friedmann-Lemaître-Robertson-Walker (FLRW) metric:

$$ds^2 = -dt^2 + a^2(t) \left[ \frac{dr^2}{1 - kr^2} + r^2(d\theta^2 + \sin^2 \theta d\phi^2) \right] \quad (18)$$

where  $t$  is time and  $(r, \theta, \phi)$  are the usual spherical coordinates. In this metric, the total symmetry in the spatial coordinates reflects the homogeneous and isotropic properties of the universe. The most important feature in the metric is that it has included a scale factor  $a(t)$  which will account for the isotropic expansion of the universe, and the constant  $k = -1, 0, 1$  corresponds to an open, flat or closed metric respectively.

In our modified theory of gravity, Einstein's equations are put in a form of field theory by the given action (15). As in the case of General Relativity, we assume a convenient form of metric that is justifiable by the assumed isotropic property of the universe. In this case, we consider a metric of the following form [5]:

$$ds^2 = \tilde{g}_{AB} dx^A dx^B = g_{\mu\nu} dx^\mu dx^\nu + b^2 dy^2 \quad (19)$$

where  $y$  is the coordinate of the fifth dimension. For simplicity, we assume that the brane is located on  $y = 0$ .

To find a cosmological solution, we further assume a maximally symmetric metric just like the FLRW metric:

$$ds^2 = -n^2(\tau, y)d\tau^2 + a^2(\tau, y)\gamma_{ij}dx^i dx^j + b^2(\tau, y)dy^2 \quad (20)$$

$\gamma_{ij}$  is the usual 3-dimensional maximally symmetric metric as seen in the FLRW metric (1). Hence our metric takes the form of

$$ds^2 = -n^2(\tau, y)d\tau^2 + a^2(\tau, y) \left[ \frac{dr^2}{1 - kr^2} + r^2(d\theta^2 - \sin^2 \theta d\phi^2) \right] + b^2(\tau, y)dy^2 \quad (21)$$

## 2.4 Einstein's Equations

As mentioned in Section 2.3, the Einstein's equations are incorporated in the action (15) as in many cosmological models. To recover the equations, we take the variation of the action (15):

$$\begin{aligned} \delta S_{(5)} = & -\frac{1}{2\kappa^2} \int d^5 X \sqrt{-\tilde{g}} (\tilde{R}_{AB} - \frac{1}{2} \tilde{R} \tilde{g}_{AB}) \delta \tilde{g}^{AB} + \int d^5 X \frac{1}{2} \sqrt{-\tilde{g}} \tilde{T}_{AB} \delta \tilde{g}^{AB} \\ & - \frac{1}{2\mu^2} \int d^4 X \sqrt{-g} (R_{\mu\nu} - \frac{1}{2} R g_{\mu\nu}) \delta g^{\mu\nu} \end{aligned} \quad (22)$$

where  $T_{\mu\nu}$  is the usual energy-momentum tensor that comes from the variation of the matter lagrangian term:

$$\tilde{T}_{AB} = \frac{2}{\sqrt{-\tilde{g}}} \left[ \frac{\delta(\sqrt{-\tilde{g}} L_m)}{\delta \tilde{g}^{AB}} - \left( \frac{\delta(\sqrt{-\tilde{g}} L_m)}{\delta \tilde{g}_{,\alpha}^{AB}} \right)_{,\alpha} \right] \quad (23)$$

Note that the variation of the 5D and 4D Hilbert-Einstein actions gives rise to the respective Einstein's tensors. By ingeniously including an extra 4D Hilbert-Einstein term in the action and hence an extra 4D Einstein's tensor in the equation, and as we are going to see later the DGP model has found a way to maintain a 4D gravity on scales smaller than the crossover scale.

Just like in the derivation of Einstein's equations in General Relativity, we have to combine the terms into one integration to reach the final conclusion. Using the following

expressions,

$$\begin{aligned}\sqrt{-g} &= \sqrt{\frac{-\tilde{g}}{b^2}} = \frac{1}{b} \sqrt{-\tilde{g}} \\ \delta g^{\mu\nu} &= \delta(\partial^\mu X_A \partial^\nu X_B \tilde{g}^{AB}) = \partial^\mu X_A \partial^\nu X_B \delta \tilde{g}^{AB} \\ \int d^4x &= \int d^5X \delta(y)\end{aligned}\tag{24}$$

we can then combine the terms of Equation (22) into one integration:

$$\begin{aligned}\delta S_{(5)} &= \int d^5X \sqrt{-\tilde{g}} \\ &\times \left[ -\frac{1}{2\kappa^2} (\tilde{R}_{AB} - \frac{1}{2} \tilde{R} \tilde{g}_{AB}) + \frac{1}{2} \tilde{T}_{AB} - \frac{\delta(y)}{2\mu^2 b} (R_{\mu\nu} - \frac{1}{2} R g_{\mu\nu}) \partial^\mu X_A \partial^\nu X_B \right] \delta \tilde{g}^{AB}\end{aligned}\tag{25}$$

Since  $\delta S_{(5)} = 0$  for arbitrary  $\delta \tilde{g}$ , the terms inside the integration must sum up to zero, so we have the modified Einstein's equations:

$$\tilde{G}_{AB} \equiv \tilde{R}_{AB} - \frac{1}{2} \tilde{R} \tilde{g}_{AB} = \kappa^2 (\tilde{T}_{AB} + \tilde{U}_{AB}) \equiv \kappa^2 \tilde{S}_{AB}\tag{26}$$

where we have introduced a new term  $\tilde{U}_{AB}$  to account for the extra terms originated from 4D scalar curvature term in the action (15):

$$\tilde{U}_{AB} = -\frac{\delta(y)}{\mu^2 b} (R_{\mu\nu} - \frac{1}{2} R g_{\mu\nu}) \partial^\mu X_A \partial^\nu X_B\tag{27}$$

In essence, the action can be split into a bulk part and a brane part and the standard calculation follows. Note that in our calculations, we choose to regard the scalar curvature term as an extra source term,  $\tilde{U}_{AB}$ , by putting it on the right-hand-side of the equation (26).

## 2.5 Energy-Momentum Tensor

Finally, we have our modified Einstein's equations, and it is time to look into each individual term of the tensor equation. First we start with the source terms  $\tilde{T}_{AB}$  and  $\tilde{U}_{AB}$ . For the energy-momentum tensor, we have contributions from both the bulk and the brane:

$$\tilde{T}_B^A = \tilde{T}_B^A|_{bulk} + \tilde{T}_B^A|_{brane}\tag{28}$$

Recall that for a homogeneous cosmic fluid, the energy-momentum tensor takes the following form:

$$T_B^A = \text{diag}(-\rho, P, P, P, P) \quad (29)$$

where  $\rho$  is the energy density of the fluid and  $P$  is the pressure. In the bulk, we assume only the contribution of a cosmological constant, thus we have  $P_B = -\rho_B$  with an equation of state  $w_B = P_B/\rho_B = -1$ . Hence, the bulk energy-momentum tensor is

$$\tilde{T}_B^A|_{\text{bulk}} = \text{diag}(-\rho_B, -\rho_B, -\rho_B, -\rho_B, -\rho_B) \quad (30)$$

In the brane, we only consider homogeneous fluids. Since the fluids are restricted to the brane, they are only 4-dimensional. We also assume that there is no flow of matter along the fifth dimension [5], thus we have  $\tilde{T}_{05} = 0$ . So the brane energy-momentum tensor is simply

$$\tilde{T}_B^A|_{\text{brane}} = \frac{\delta(y)}{b} \text{diag}(-\rho_b, p_b, p_b, p_b, 0) \quad (31)$$

## 2.6 Scalar Curvature Source Term $\tilde{U}$

As mentioned in Section 2.4,  $\tilde{U}$  is the 4D Einstein tensor regarded as a source term, so to calculate this scalar curvature term introduced in Equation (26), we only need to calculate the 4D tensors restricted to the brane,  $R_{\mu\nu}$ , and  $R$ . From the metric (20), we find the restricted 4D metric in the brane as follows

$$ds^2 = -n^2 d\tau^2 + a^2 \left( \frac{dr^2}{1 - kr^2} + r^2 (d\theta^2 + \sin^2 \theta d\phi^2) \right) \quad (32)$$

This is similar to a standard 4D isotropic metric with the exception of a dynamical cosmic time.

From the metric, we calculate the Christoffel symbols using the formula from General Relativity:

$$\Gamma_{\mu\nu}^\rho = \frac{1}{2} g^{\rho\lambda} (g_{\lambda\mu,\nu} + g_{\lambda\nu,\mu} - g_{\mu\nu,\lambda}) \quad (33)$$

After calculations, we get:

$$\begin{aligned} \Gamma_{00}^0 &= \frac{\dot{n}}{n} & \Gamma_{00}^i &= 0 \\ \Gamma_{0i}^0 &= 0 & \Gamma_{0j}^i &= \frac{\dot{a}}{a} \delta_j^i \\ \Gamma_{ij}^0 &= \frac{a\dot{a}}{n^2} \gamma_{ij} & \Gamma_{jk}^i &= \frac{1}{2} \gamma^{im} (\gamma_{mj,k} + \gamma_{mk,j} - \gamma_{jk,m}) \end{aligned} \quad (34)$$

We will be using spherical spatial coordinates  $(r, \theta, \phi)$  in the calculation, and the non-zero  $\Gamma_{jk}^i$ 's in the equation above are:

$$\begin{aligned}\Gamma_{11}^1 &= \frac{kr}{1-kr^2} & \Gamma_{12}^2 &= \frac{1}{r} & \Gamma_{13}^3 &= \frac{1}{r} \\ \Gamma_{22}^1 &= -r(1-kr^2) & \Gamma_{33}^2 &= -\sin\theta\cos\theta & \Gamma_{23}^3 &= \cot\theta \\ \Gamma_{33}^1 &= -r\sin^2\theta(1-kr^2)\end{aligned}\quad (35)$$

From the Christoffel symbols, we calculate the Ricci tensor using the usual formula from General Relativity again:

$$R_{\mu\nu} = \Gamma_{\mu\nu,\lambda}^\lambda - \Gamma_{\mu\lambda,\nu}^\lambda + \Gamma_{\alpha\lambda}^\lambda \Gamma_{\mu\nu}^\alpha - \Gamma_{\alpha\mu}^\lambda \Gamma_{\lambda\nu}^\alpha \quad (36)$$

The non-zero terms are

$$\begin{aligned}R_{00} &= -3\frac{\ddot{a}}{a} + 3\frac{\dot{a}\dot{n}}{an} \\ R_{ij} &= \left( \frac{a\ddot{a}}{n^2} + 2\frac{\dot{a}^2}{n^2} - \frac{a\dot{a}\dot{n}}{n^3} + 2k \right) \gamma_{ij}\end{aligned}\quad (37)$$

By contracting the Ricci tensor, we get the Ricci scalar

$$R = 6 \left( \frac{\ddot{a}}{an^2} + \frac{\dot{a}^2}{a^2n^2} - \frac{\dot{a}\dot{n}}{an^3} + \frac{k}{a^2} \right) \quad (38)$$

Finally, we calculate the non-zero terms of  $\tilde{U}_{\mu\nu}$ . From Equation (27),

$$\tilde{U}_{\mu\nu} = -\frac{\delta(y)}{\mu^2 b} \left( R_{\mu\nu} - \frac{1}{2} R g_{\mu\nu} \right) \quad (39)$$

and the non-zero terms are

$$\begin{aligned}\tilde{U}_{00} &= -\frac{3\delta(y)}{\mu^2 b} \left( \frac{\dot{a}^2}{a^2} + k \frac{n^2}{a^2} \right) \\ \tilde{U}_{ij} &= -\frac{\delta(y)}{\mu^2 b} \left[ \frac{a^2}{n^2} \left( -\frac{\dot{a}^2}{a^2} + 2\frac{\dot{a}\dot{n}}{an} - 2\frac{\ddot{a}}{a} \right) - k \right] \gamma_{ij}\end{aligned}\quad (40)$$



## 2.7 First Integral of Einstein's Equations in the Bulk

After looking at the source terms  $\tilde{T}$  and  $\tilde{U}$  on the right-hand-side of Einstein's equations, we will now look at the left-hand-side. Using the full metric (20), we can do a similar calculation of the bulk Christoffel symbols using Equation (33) again, bearing in mind that the variables are now functions of both time,  $\tau$  and the extra dimension,  $y$ . Here  $\dot{a}$  denotes a differentiation with respect to time, while  $a'$  denotes a differentiation with respect to  $y$ :

$$\begin{aligned}
\Gamma_{00}^0 &= \frac{\dot{n}}{n} & \Gamma_{00}^i &= 0 & \Gamma_{00}^5 &= \frac{nn'}{b^2} \\
\Gamma_{0i}^0 &= 0 & \Gamma_{0j}^i &= \frac{\dot{a}}{a} \delta_j^i & \Gamma_{0i}^5 &= 0 \\
\Gamma_{05}^0 &= \frac{n'}{n} & \Gamma_{05}^i &= 0 & \Gamma_{05}^5 &= \frac{\dot{b}}{b} \\
\Gamma_{ij}^0 &= \frac{a\dot{a}}{n^2} \gamma_{ij} & \Gamma_{jk}^i &= \frac{1}{2} \gamma^{im} (\gamma_{mj,k} + \gamma_{mk,j} - \gamma_{jk,m}) & \Gamma_{ij}^5 &= -\frac{aa'}{b^2} \gamma_{ij} \\
\Gamma_{i5}^0 &= 0 & \Gamma_{j5}^i &= \frac{a'}{a} \delta_j^i & \Gamma_{i5}^5 &= 0 \\
\Gamma_{55}^0 &= \frac{b\dot{b}}{n^2} & \Gamma_{55}^i &= 0 & \Gamma_{55}^5 &= \frac{b'}{b}
\end{aligned} \tag{41}$$

Note that the terms involving only the 4 usual dimensions are exactly the same as the corresponding terms in the restricted version we calculated in Section 2.6. We can also see that there is a symmetry between the terms involving 0 and 5, since they are the only two variables we are differentiating with respect to.

From the Christoffel symbols, we get the terms for the bulk Ricci tensor using the same Equation (36) as in the previous section:

$$\begin{aligned}
\tilde{R}_{00} &= \frac{nn''}{b^2} - \frac{nn'b'}{b^3} - 3\frac{\ddot{a}}{a} - \frac{\ddot{b}}{b} + 3\frac{\dot{a}\dot{n}}{an} + \frac{\dot{b}\dot{n}}{bn} + 3\frac{nn'a'}{ab^2} \\
\tilde{R}_{ij} &= \left( \frac{a\ddot{a}}{n^2} + 2\frac{\dot{a}^2}{n^2} - \frac{a\dot{a}\dot{n}}{n^3} - \frac{aa''}{b^2} - 2\frac{a'^2}{b^2} + \frac{aa'b'}{b^3} + \frac{a\dot{a}\dot{b}}{n^2b} - \frac{aa'n'}{b^2n} + 2k \right) \gamma_{ij} \\
\tilde{R}_{55} &= \frac{b\ddot{b}}{n^2} - \frac{b\dot{b}\dot{n}}{n^3} - \frac{n''}{n} - 3\frac{a''}{a} + 3\frac{b\dot{b}\dot{a}}{an^2} + \frac{b'n'}{bn} + 3\frac{a'b'}{ab} \\
\tilde{R}_{05} &= -3 \left( \frac{\dot{a}'}{a} - \frac{\dot{a}n'}{an} - \frac{a'\dot{b}}{ab} \right)
\end{aligned} \tag{42}$$

As usual, we can then contract the Ricci tensor to get the Ricci scalar:

$$\begin{aligned}
\tilde{R} &= 2 \left( -\frac{n''}{b^2n} + \frac{n'b'}{b^3n} + \frac{\ddot{b}}{bn^2} - \frac{\dot{b}\dot{n}}{bn^3} \right) \\
&\quad + 6 \left( \frac{\ddot{a}}{an^2} - \frac{\dot{a}\dot{n}}{an^3} - \frac{a''}{ab^2} + \frac{a'b'}{ab^3} - \frac{a'n'}{anb^2} + \frac{\dot{a}\dot{b}}{abn^2} + \frac{\dot{a}^2}{a^2n^2} - \frac{a'^2}{a^2b^2} + \frac{k}{a^2} \right)
\end{aligned} \tag{43}$$

We can use the Ricci tensor to calculate the Einstein's tensor from Equation (26):

$$\begin{aligned}
\tilde{G}_{00} &= 3 \left( \frac{\dot{a}^2}{a^2} + \frac{\dot{a}\dot{b}}{ab} - \frac{a''n^2}{ab^2} + \frac{a'b'n^2}{ab^3} - \frac{a'^2n^2}{a^2b^2} + \frac{kn^2}{a^2} \right) \\
\tilde{G}_{ij} &= \left[ \frac{a^2}{b^2} \left( 2\frac{a''}{a} + \frac{n''}{n} + \frac{a'^2}{a^2} + 2\frac{a'n'}{an} - 2\frac{a'b'}{ab} - \frac{b'n'}{bn} \right) \right. \\
&\quad \left. - \frac{a^2}{n^2} \left( 2\frac{\ddot{a}}{a} + \frac{\ddot{b}}{b} + \frac{\dot{a}^2}{a^2} - 2\frac{\dot{a}\dot{n}}{an} + 2\frac{\dot{a}\dot{b}}{ab} - \frac{\dot{b}\dot{n}}{bn} \right) - k \right] \gamma_{ij} \\
\tilde{G}_{55} &= 3 \left( \frac{a'^2}{a^2} + \frac{a'n'}{an} - \frac{b^2\ddot{a}}{an^2} + \frac{b^2\dot{a}\dot{n}}{an^3} - \frac{b^2\dot{a}^2}{a^2n^2} - \frac{kb^2}{a^2} \right) \\
\tilde{G}_{05} &= -3 \left( \frac{\dot{a}'}{a} - \frac{\dot{a}n'}{an} - \frac{a'\dot{b}}{ab} \right)
\end{aligned} \tag{44}$$

Since the Einstein tensor involves only the 5D metric, it is the same as in the case of a normal 5D braneworld model without the extra 4D term [8]. The contributions of the 4D scalar curvature terms are all contained in  $\tilde{U}_{AB}$ .

Now that we have established the full Einstein's equations (26), we can look for some useful equations out of those lengthy ones. If we look at the (05) term of Einstein's equations (26), we have

$$\tilde{G}_{05} = -3 \left( \frac{\dot{a}'}{a} - \frac{\dot{a}n'}{an} - \frac{a'\dot{b}}{ab} \right) = \kappa^2(\tilde{T}_{05} + \tilde{U}_{05}) = 0 \tag{45}$$

We define the following function of  $\tau$  and  $y$  only:

$$F(\tau, y) = \frac{(a'a)^2}{b^2} - \frac{(\dot{a}a)^2}{n^2} - ka^2 \tag{46}$$

We can proceed to calculate the derivatives of  $F$  with respect to  $\tau$  and  $y$ :

$$\begin{aligned}
F' &= \frac{2a'a(a''a + a'^2)}{b^2} - \frac{2(a'a)^2b'}{b^3} - \frac{2\dot{a}a(\dot{a}'a + a'\dot{a})}{n^2} + \frac{2(\dot{a}a)^2n'}{n^3} - 2kaa' \\
&= -\frac{2a^3a'}{n^2} \left( \frac{\dot{a}^2}{a^2} + \frac{\dot{a}\dot{b}}{ab} - \frac{a''n^2}{ab^2} + \frac{a'b'n^2}{ab^3} - \frac{a'^2n^2}{a^2b^2} + \frac{kn^2}{a^2} \right) - \frac{2a^3\dot{a}}{n^2} \left( \frac{\dot{a}'}{a} - \frac{\dot{a}n'}{an} - \frac{a'\dot{b}}{ab} \right) \\
&= -\frac{2a^3a'}{3n^2} \tilde{G}_{00}
\end{aligned} \tag{47}$$

where in the last equality, we have used Equation (45); similarly for  $\dot{F}$ , we have:

$$\begin{aligned}\dot{F} &= \frac{2a'a(\dot{a}'a + a'\dot{a})}{b^2} - \frac{2(a'a)^2\dot{b}}{b^3} - \frac{2\dot{a}a(\ddot{a}a + \dot{a}^2)}{n^2} - \frac{2(\dot{a}a)^2\dot{n}}{n^3} - 2ka\dot{a} \\ &= \frac{2a^3\dot{a}}{b^2} \left( \frac{a'^2}{a^2} + \frac{a'n'}{an} - \frac{b^2\ddot{a}}{an^2} + \frac{b^2\dot{a}\dot{n}}{an^3} - \frac{b^2\dot{a}^2}{a^2n^2} - \frac{kb^2}{a^2} \right) + \frac{2a^3a'}{b^2} \left( \frac{\dot{a}'}{a} - \frac{\dot{a}n'}{an} - \frac{a'\dot{b}}{ab} \right) \\ &= \frac{2a^3\dot{a}}{3b^2} \tilde{G}_{55}\end{aligned}\quad (48)$$

On the other hand, if we look at the (55) term of Einstein's equations (26):

$$\tilde{G}_{55} = \kappa^2(\tilde{T}_{55} + \tilde{U}_{55}) = -\kappa^2\rho_B b^2 \quad (49)$$

Then Equation (48) becomes

$$\dot{F} = -\frac{2}{3}\kappa^2 a^3 \dot{a} \rho_B \quad (50)$$

Furthermore, by exploiting the fact that the bulk energy density is assumed to be constant (coming from only the contribution of a cosmological constant), we can integrate the equation and get

$$F = -\frac{1}{6}\kappa^2 a^4 \rho_B - C \quad (51)$$

where  $C$  is the integration constant.

Finally, we get the first integral form of the Einstein's equations by substituting in the expression of  $F$  (46):

$$\frac{(a'a)^2}{b^2} - \frac{(\dot{a}a)^2}{n^2} - ka^2 + \frac{\kappa^2}{6}a^4\rho_B + C = 0 \quad (52)$$

Again, because  $\tilde{U}_{AB}$  is only brane-related and does not contribute in the calculations above, this equation is the same as in the case of a normal 5D braneworld model [8]. In the next section, we will see that this changes when we calculate the Friedmann equations that take contributions from all dimensions.

### 3 Friedmann Equations and the Cosmology of DGP Model

#### 3.1 Friedmann Equations

In Section 2, we have talked about the Einstein's equations as the equation governing the gravitational interactions of masses and energies, but we need more explicit equations to better understand the evolution of the universe. For that purpose, we have the Friedmann equations.

In General Relativity, by assuming the FLRW metric (1), one can calculate the Einstein's equations (9) in an explicit form and from them, we can derive two independent equations known as the Friedmann equations [1]:

$$\begin{aligned} H^2 &\equiv \left(\frac{\dot{a}}{a}\right)^2 = \frac{8\pi G}{3}\rho - \frac{k}{a^2} \\ \frac{\ddot{a}}{a} &= -\frac{4\pi G}{3}(p + 3\rho) \end{aligned} \quad (53)$$

where all energy densities are combined into a single term  $\rho$  and the Hubble parameter,  $H = \dot{a}/a$ , is introduced to measure the rate of expansion of the universe. From these equations, we can derive the evolution of the scale factor  $a(t)$  which represents the expansion directly. On the other hand, we can also derive the equation of continuity from the Friedmann equations:

$$\dot{\rho} + 3(p + \rho)\frac{\dot{a}}{a} = 0 \quad (54)$$

This equation has the similar significance as in fluid dynamic. In our case, the equation represents the conservation of energy of the cosmic fluid in the universe. If we further assume a constant equation of state  $w = p/\rho$ , the equation of continuity becomes:

$$\dot{\rho} + 3(w + 1)\rho\frac{\dot{a}}{a} = 0 \quad (55)$$

If we arrange the terms and integrate both sides, we will get:

$$\begin{aligned} \frac{\dot{\rho}}{\rho} &= -3(w + 1)\frac{\dot{a}}{a} \\ \ln \rho &= -3(w + 1) \ln a + C \\ \rho &\propto a^{-3(w+1)} \end{aligned} \quad (56)$$

where  $C$  is the integration constant.

When we discuss the topic of cosmology, and especially the observation parts, one of the important concepts that must to be understood is the red-shift. Because of the on-going expansion of the universe, the wavelength of an emission from a distant source would have increased when it reaches earth, this phenomenon is known as the red-shift, for shifting towards the longer wavelengths. More precisely, the red-shift,  $1 + z = \lambda_0/\lambda$ , is defined as the ratio of the measured wavelength,  $\lambda_0$ , over the original wavelength,  $\lambda$ . Alternatively, the red-shift can also be defined as  $1 + z = a_0/a$ , which is the ratio of the scale factor of today,  $a_0$  over the scale factor at the time of emission,  $a$ . It is clear from the alternative definition that the red-shift  $z$  can be used as a measure of time, but it can also be used as a measure of distance if we multiply it by the speed of light. In observations, these two concepts are closely related. With the introduction of  $z$ , we can further simplify Equation (56):

$$\frac{\rho}{\rho_0} = \left(\frac{a}{a_0}\right)^{-3(w+1)} = (1+z)^{3(w+1)} \quad (57)$$

where  $\rho_0$  is the current value of the energy density. This equation is the equation of evolution for the energy densities with a constant equation of state, for example matter or dust ( $w = 0$ ), light ( $w = 1/3$ ) and the cosmological constant ( $w = -1$ ). The differential equation is linear, so it is possible to have different energy densities in the system and the total energy density is simply given by:

$$\rho(z) = \sum_i \rho_0^{(i)} (1+z)^{3(w_i+1)} \quad (58)$$

where  $\rho_0^{(i)}$  are the respective energy densities of today.

To further simplify the equations using dimensionless quantities, the density parameter,  $\Omega(t) \equiv \rho(t)/\rho_c(t)$ , is introduced, where  $\rho_c(t) = 3H^2(t)/8\pi G$ , known as the critical density, is the total density corresponding to a flat universe. With these definitions, the first Friedmann equation becomes (53):

$$1 = \Omega(t) - \frac{k}{a^2 H^2(t)} \quad (59)$$

It is clear from the above equation that the flatness of the universe depends on the total energy density of its content and  $\Omega(t) = 1$  corresponds to a flat universe. Since we can well measure the current energy content of the universe, it is favorable to put the equation in

comparison with the current energy density:

$$\frac{H^2(t)}{H_0^2} = \frac{\rho(t)}{\rho_c^{(0)}} - \frac{k}{a^2 H_0^2} \quad (60)$$

where  $H_0$  is the Hubble parameter of current time. In terms of the red-shift, we have:

$$\frac{H^2(z)}{H_0^2} = \sum_i \frac{\rho_0^{(i)}}{\rho_c^{(0)}} (1+z)^{3(w_i+1)} - \frac{k}{a_0^2 H_0^2} (1+z)^2 \quad (61)$$

where we have split the total energy density into different components and replace  $a$  with  $a_0/(1+z)$ . As a conclusion, the first Friedmann equation that has been derived from the  $\Lambda$ CDM model by assuming a FLRW metric can be presented in a simple form:

$$H^2(z) = H_0^2 [\Omega_k (1+z)^2 + \Omega_M (1+z)^3 + \Omega_X (1+z)^{3(1+w_X)}] \quad (62)$$

where  $\Omega_M = \rho_0^{(M)}/\rho_c^{(0)}$  is the current density parameter for matter,  $\Omega_X = \rho_0^{(X)}/\rho_c^{(0)}$  is the current density parameter for dark energy with the equation of state  $w_X$  and  $\Omega_k = -\frac{k}{a_0^2 H_0^2}$  is an artificial term that represents the flatness of the universe. Note that when the equation is evaluated at  $z = 0$  which is today, we have:

$$\Omega_k + \Omega_M + \Omega_X = 1 \quad (63)$$

In other words, the current density parameters have to add up to 1 if the flatness term is included. This is known as the normalization condition and it is used as one of the constraints in adjusting the parameters for the  $\Lambda$ CDM model. When  $\Omega_k = 0$  or, equivalently, the universe is flat, the current total density parameter is 1 and recent observations suggest that this is indeed the case.

### 3.2 Junction Conditions for DGP Model

After looking at the Friedmann equations for General Relativity, we can now turn our attention back to our DGP model. The goal of this section is to solve the Einstein equations (26) around  $y = 0$  to get the equation of motion in the brane. When solving differential equations, we need to first define the boundary conditions. In our case, we have to deal with the junction condition on connecting the brane and the bulk metric. In order to have a well-defined geometry, the scale factor  $a$  is required to be continuous at  $y = 0$ , but it is not necessarily smooth. In the case when  $a$  is not-smooth,  $a'$  will be discontinuous [9], and

$a''$  will have a corresponding delta distribution to account for the discontinuity:

$$a'' = \hat{a}'' + [a']\delta(y) \quad (64)$$

where  $\hat{a}''$  is the continuous part of  $a''$  and  $[a']$  is the jump of  $a'$ . If we substitute the expression of  $a''$  (64) into the Einstein's tensor (44), compare it to  $\tilde{T}$  and  $\tilde{U}$  and equate the terms containing  $\delta(y)$ , then from the  $\tilde{G}_{00}$  term we get:

$$-3\frac{[a']n^2}{ab^2} = \kappa^2(\tilde{T}_{00} + \tilde{U}_{00}) = \kappa^2 n^2 \frac{\rho_b}{b} - \frac{3\kappa^2}{\mu^2 b} \left( \frac{\dot{a}^2}{a^2} + k \frac{n^2}{a^2} \right) \quad (65)$$

Similarly, we can also have a jump in  $n'$ , which gives us the expression of  $n''$ :

$$n'' = \hat{n}'' + [n']\delta(y) \quad (66)$$

Again we substitute the expressions of  $a''$  and  $n''$  into the Einstein's equation and consider only the  $\delta(y)$  terms, then from the  $\tilde{G}_{11}$  term we get:

$$\begin{aligned} \frac{a^2}{b^2} \left( 2\frac{[a']}{a} + \frac{[n']}{n} \right) \gamma_{11} &= \kappa^2(\tilde{T}_{11} + \tilde{U}_{11}) \\ &= -\kappa^2 a^2 \gamma_{11} \frac{p_b}{b} - \frac{\kappa^2}{\mu^2 b} \left[ \frac{a^2}{n^2} \left( -\frac{\dot{a}^2}{a^2} + 2\frac{\dot{a}^2 \dot{n}^2}{a^2 n^2} - 2\frac{\ddot{a}}{a} \right) - k \right] \gamma_{11} \end{aligned} \quad (67)$$

We can combine them and get the following junction conditions:

$$\begin{aligned} \frac{[a']}{a_0 b_0} &= -\frac{\kappa^2}{3} \rho_b + \frac{\kappa^2}{\mu^2 n_0^2} \left( \frac{\dot{a}_0^2}{a_0^2} + k \frac{n_0^2}{a_0^2} \right) \\ \frac{[n']}{n_0 b_0} &= \frac{\kappa^2}{3} (3p_b + 2\rho_b) + \frac{\kappa^2}{\mu^2 n_0^2} \left( 2\frac{\ddot{a}_0}{a_0} - \frac{\dot{a}_0^2}{a_0^2} - 2\frac{\dot{a}_0 \dot{n}_0}{a_0 n_0} - k \frac{n_0^2}{a_0^2} \right) \end{aligned} \quad (68)$$

where  $a_0$  and  $n_0$  are  $a$  and  $n$  restricted to the brane ( $y = 0$ ), respectively.

We can see in the Einstein's equations, in the expression of  $\tilde{U}$  in particular, as well as in the formula above, that the 4D curvature term plays the role of a source term. In Deffayet's paper, he formulated a fictitious cosmic fluid to represent the effect of the 4D scalar curvature term in the action [5]. The properties of the fluid are given by

$$\begin{aligned} \rho_{curv} &= -\frac{3}{\mu^2 n_0^2} \left( \frac{\dot{a}_0^2}{a_0^2} + k \frac{n_0^2}{a_0^2} \right) \\ p_{curv} &= \frac{1}{\mu^2 n_0^2} \left( 2\frac{\ddot{a}_0}{a_0} + \frac{\dot{a}_0^2}{a_0^2} - 2\frac{\dot{a}_0 \dot{n}_0}{a_0 n_0} + k \frac{n_0^2}{a_0^2} \right) \end{aligned} \quad (69)$$

Whilst this interpretation gives a clear view of how the extra term in the action can be interpreted mathematically as another source term, we have to be careful not to over interpret this term because, as we will see later, this term contains terms of  $H$ , and it is not the same as a regular density in the Friedmann equations.

Looking back at the junction condition (68), by assuming a  $y$  to  $-y$  symmetry, we have  $[a'] = 2a'(0+)$ . When  $y \rightarrow 0$ , we combine the integrated Einstein's equation (52) and the junction condition (68) to get the first Friedmann-like equation:

$$\epsilon \sqrt{H^2 - \frac{\kappa^2}{6} \rho_B - \frac{C}{a_0^4} + \frac{k}{a_0^2}} = \frac{\kappa^2}{2\mu^2} \left( H^2 + \frac{k}{a_0^2} \right) - \frac{\kappa^2}{6} \rho_b \quad (70)$$

where  $H = \frac{\dot{a}_0}{a_0 n_0}$  and  $\epsilon$  is the sign of  $[a']$ . This is the equation that governs the dynamics of the cosmology, particularly the evolution of the Hubble parameter,  $H$ .

On the other hand, by substituting the junction conditions into the (05) term of Einstein's equations (45), we can recover the usual continuity equation:

$$\dot{\rho}_b + 3(p_b + \rho_b) \frac{\dot{a}_0}{a_0} = 0 \quad (71)$$

This is important because from this equation, and by assuming a constant equation of state for the fluids, we get the usual evolution of densities:  $\rho \propto a^{-3(1+w)}$ , even in the DGP model. This idea will be used to express the Hubble parameter in terms of the relative density parameter.

### 3.3 5D Cosmology

After developing the equations of evolution, we can have some qualitative discussions on the cosmology of the DGP model. The first thing we notice from the Friedmann-like equation is that we can recover the full 5D regime, i.e. without the 4D curvature term, simply by letting  $\mu \rightarrow \infty$ . If we set the integration constant  $C$  and the bulk cosmological constant  $\rho_B$  to zero, we get

$$H^2 + \frac{k}{a_0^2} = \frac{\kappa^4}{36} \rho_b^2 \quad (72)$$

We can see from the normal 5D Friedmann equation above that the 5D gravity is indeed different from the 4D gravity, which has  $H^2 \propto \rho$ . It is important to show that the Friedmann equation of the DGP model will be more like a 4D one on observational scales.



### 3.4 Recovery of Standard Cosmology

If we were to accept this model, the most basic requirement is the model has to agree with current observations, so the next natural topic is to show that we can recover the standard cosmology under some specific conditions [5]. In the following discussion, we set  $C = 0$  and  $\rho_B = 0$ .

We begin by rewriting the first Friedmann equation (70) into a more convenient form:

$$\frac{\mu^2}{3}\rho_b = H^2 + \frac{k}{a_0^2} - 2\epsilon\frac{\mu^2}{\kappa^2}\sqrt{H^2 + \frac{k}{a_0^2}} \quad (73)$$

If we compare the equation with the corresponding equation for standard cosmology:

$$\frac{8\pi G_{(4)}}{3}\rho_b = H^2 + \frac{k}{a_0^2} \quad (74)$$

it is clear that the standard equation can be recovered under the following condition:

$$\sqrt{H^2 + \frac{k}{a_0^2}} \gg 2\frac{\mu^2}{\kappa^2} \quad (75)$$

If we assume a flat universe ( $k = 0$ ), then the condition (75) becomes

$$H^{-1} \ll \frac{M_{(4)}^2}{2M_{(5)}^3} = r_c \quad (76)$$

This is consistent with our interpretation of the cross-over scale. In other words, if the current Hubble radius is much smaller than the cross-over scale, then all measurements and observations within this scale will only measure in effect the 4D gravity and will not be able to detect the extra dimension.

### 3.5 Late-time Cosmology

After showing that the DGP model can be undetectable under the current observations, we can further explore the cosmology of the model by looking at the late-time cosmology. In cosmology, one topic of interest is the future development of our universe. We are interested to see whether the current phase of accelerating expansion is long-lasting or just transient. To see this, we have to go back to the Friedmann equation. We begin by rewriting the first

Friedmann equation (73) in a more convenient form. If we solve for  $\sqrt{H^2 + \frac{k}{a_0^2}}$ , we will get

$$\sqrt{H^2 + \frac{k}{a_0^2}} = \epsilon \frac{\mu^2}{\kappa^2} \pm \sqrt{\frac{\mu^2}{3} \rho_b + \frac{\mu^4}{\kappa^4}} \quad (77)$$

Note that in the most general scenario, we allow  $\rho_b$  to be negative, that is to allow the possibility of a negative brane cosmological constant. In that case, both the plus and the minus solutions are admissible regardless of the sign of  $\epsilon$ .

Depending on the sign of  $\epsilon$ , the equation has two separate branches of solutions [5][6]. In the first scenario, we have

$$\begin{aligned} \epsilon &= -1 \\ k &= 0 \text{ or } k = -1 \end{aligned} \quad (78)$$

In this case, Equation (77) has to take the form

$$\sqrt{H^2 + \frac{k}{a_0^2}} = -\frac{\mu^2}{\kappa^2} + \sqrt{\frac{\mu^2}{3} \rho_b + \frac{\mu^4}{\kappa^4}} \quad (79)$$

This will be known as the *Brane 1* solution.

Assuming the usual equations of state:

$$p_b = w \rho_b, \quad w \geq -1 \quad (80)$$

Then by integrating Friedmann's equation, we see that  $a_0$  diverges at late time, and the matter energy density goes to zero:

$$a_0 \rightarrow \infty, \quad \rho_m \rightarrow 0 \quad (81)$$

Note that the first Friedmann equation (79) in this scenario takes the form of

$$\sqrt{H^2 + \frac{k}{a_0^2}} = \frac{\mu^2}{\kappa^2} \left( -1 + \sqrt{1 + \frac{\rho_b}{3 \frac{\mu^2}{\kappa^4}}} \right) \quad (82)$$

Since matter density is going to zero, it will eventually reach a time when  $\rho_b \ll \frac{\mu^2}{\kappa^4}$ . Then in the first order approximation, we can expand the square-root term:

$$\sqrt{1 + \frac{\rho_b}{3 \frac{\mu^2}{\kappa^4}}} = 1 + \frac{1}{2} \frac{\rho_b}{3 \frac{\mu^2}{\kappa^4}} = 1 + \frac{1}{6} \frac{\kappa^4 \rho_b}{\mu^2} \quad (83)$$

and the Friedmann equation (82) can be simplified to

$$\sqrt{H^2 + \frac{k}{a_0^2}} = \frac{1}{6}\kappa^2\rho_b \quad (84)$$

Hence we have a transition to the fully 5D regime (cf. Equation (72)). We also see that the condition  $\rho_b \ll \frac{\mu^2}{\kappa^4}$  is equivalent to  $\sqrt{H^2 + \frac{k}{a_0^2}} \ll r_c^{-1}$ , which in a flat universe becomes  $H^{-1} \gg r_c$ , and that turns out to be our initial condition for transition into the 5D cosmology.

In our second scenario, we assume

$$\epsilon = 1 \quad (85)$$

In this case, the Friedmann equation can still have two solutions, but it is easy to see that the ‘-’ branch has the same features as the *Brane 1* solution, but with different constraints on the parameters. The two cases will be grouped together and be collectively known as the *Brane 1* solution while the ‘+’ branch with a different feature will be known as the *Brane 2* solution:

$$\sqrt{H^2 + \frac{k}{a_0^2}} = \frac{\mu^2}{\kappa^2} \left( 1 + \sqrt{1 + \frac{\kappa^4 \rho_b}{3\mu^2}} \right) \geq \frac{2\mu^2}{\kappa^2} \equiv H_{self} \quad (86)$$

Note that  $H$  is bounded below by a constant  $H_{self}$ . In late time, we have

$$\begin{aligned} a_0 &\rightarrow \infty \\ H &\rightarrow H_{self} \end{aligned} \quad (87)$$

We will then have an inflationary solution with a constant  $H$ , approximately. We will refer to this solution as the self-inflationary solution.

It has been shown by Shtanov that this is not the only inflationary solution [10]. If we assume a constant  $H$ :

$$\begin{aligned} \epsilon &= 1 \\ \rho_b &= 0 \\ H &\text{ constant} \end{aligned} \quad (88)$$

and substitute the assumption into the Friedmann’s equation (70), we get the same  $H$  as

in the self-inflationary case:

$$H = \frac{2\mu^2}{\kappa^2} = H_{self} \quad (89)$$

This suggests that all inflationary solutions have the same  $H$ . On the other hand, recall that  $H = \frac{\dot{a}_0}{a_0 n_0}$ , we have

$$0 = \dot{H} = \frac{\ddot{a}_0}{a_0 n_0} - \frac{\dot{a}_0(\dot{a}_0 n_0 + a_0 \dot{n}_0)}{(a_0 n_0)^2} = \frac{\ddot{a}_0 a_0 n_0 - \dot{a}_0(\dot{a}_0 n_0 + a_0 \dot{n}_0)}{a_0^2 n_0^2} \quad (90)$$

From that, we deduce

$$\ddot{a}_0 = \frac{\dot{a}_0^2}{a_0} + \frac{\dot{a}_0 \dot{n}_0}{n_0} \quad (91)$$

Again, by assuming a flat universe ( $k = 0$ ), and from Equation (69), we have

$$\rho_{curv} = -p_{curv} = -\frac{3H^2}{\mu^2} = \text{constant} \quad (92)$$

Combining Equation (89) and Equation (92), we get an expression similar to the normal de Sitter expansion:

$$H^2 = \frac{\kappa^4}{36} \rho_{curv}^2 \quad (93)$$

We see that the intrinsic curvature term acts as a negative cosmological constant in the brane. However, we can achieve the same equation by replace the self curvature term by a positive brane tension [5]:

$$\lambda_{brane} = \rho_b = -\rho_{curv} \quad (94)$$

This will be known as the tension-inflationary solution.

We see here for the first time that there are two branches of solutions to the Friedmann equation (70). If we take the 3D brane as a boundary of the (4+1)D bulk, then these two solutions represent two different forms of the boundary [6]: the *Brane 1* solution corresponds to the case when the inner normal of the brane points in the direction of decreasing bulk coordinate, while *Brane 2* corresponds to the complementary case where the inner normal points in the increasing direction. For example, if our brane is a 3-sphere embedded in a 3-spherically-symmetric bulk, then *Brane 1* is the case where the bulk is the interior of the  $S^3$ -brane, while *Brane 2* is the case when the bulk is the exterior of the  $S^3$ -brane. In our case when the brane is assumed to be flat, the two branches correspond to the cases where the bulk is on the  $y < 0$  side (*Brane 1*) or the  $y > 0$  side (*Brane 2*).

### 3.6 Cosmology of Phantom Energy Dominated Universe

In a later paper of Shtanov [6], he also pointed out that it is possible for the DGP model to exhibit similar properties to those of phantom energy, that is to have a very negative effective equation of state ( $w_{eff} < -1$ ). This is usually unfavorable, because the corresponding ever-increasing density violates the conservation of energy. But in our model, since there is no physical fluid that actually has an equation of state of  $w < -1$ , none of the cosmic fluid densities (possibly including a cosmological constant term) diverges in late time.

A simple realization of the case of  $w_{eff} < -1$  is presented by Lue and Starkman [11]. The cosmology was derived from a *Brane 1* solution by assuming a flat universe and having only pressureless matter and a brane cosmological constant,  $\Lambda_b$ , in the brane. In this case, the Friedmann equation (79) becomes

$$\begin{aligned}
 H &= -\frac{\mu^2}{\kappa^2} + \sqrt{\frac{\mu^2}{3}\rho_M + \Lambda_b + \frac{\mu^4}{\kappa^4}} \\
 H + \frac{\mu^2}{\kappa^2} &= \sqrt{\frac{\mu^2}{3}\rho_M + \Lambda_b + \frac{\mu^4}{\kappa^4}} \\
 H^2 + 2H\frac{\mu^2}{\kappa^2} + \frac{\mu^4}{\kappa^4} &= \frac{\mu^2}{3}\rho_M + \Lambda_b + \frac{\mu^4}{\kappa^4} \\
 H^2 &= \frac{\mu^2}{3}\rho_M + \left(\Lambda_b - 2H\frac{\mu^2}{\kappa^2}\right)
 \end{aligned} \tag{95}$$

Note that in the end, we have put the equation in a form similar to a standard Friedmann equation:  $H^2 = \frac{\mu^2}{3}\rho_M + \Lambda_b$ , so we can effectively interpret the last term as an effective cosmological constant:  $\Lambda_{eff} = \Lambda_b - 2H\frac{\mu^2}{\kappa^2}$ . Since  $H$  is a decreasing function,  $\Lambda_{eff}$  is increasing with time. This shows a similar behavior to that of a phantom energy which may then give a better fit to the current observed data. The resemblance to phantom energy doesn't stop here, as we will see later in Section 4.4 that if we define an effective equation of state for this term, it turns out to be  $w_{eff} < -1$ . More detailed discussions will be given in the said section. This interesting setting is then fitted to the observations in Section 5.

### 3.7 Brane Embedding in Minkowski Space-time

Although we are mainly interested in the evolution in the brane, but for the completeness of the theory, we cannot forget about the 5D bulk. In a good theory or model, the transition

from the brane to the bulk should be smooth, so we have to contemplate on how to properly embed the brane in the bulk [5][8]. In the discussions that follow, we assume a flat or Minkowski space-time. To calculate the restricted metric, we will first consider a thin slab of the 5D universe centered around  $y = 0$ . In the metric (20), the terms to calculate are  $a(\tau, y)$ ,  $b(\tau, y)$  and  $n(\tau, y)$ . By a redefinition of  $y$ , and assuming  $b$  is independent of time, we can get

$$b_0(\tau) \equiv b(\tau, 0) = 1 \quad (96)$$

where we have used the subscript 0 to denote the values at  $y = 0$ . Then from the (05) term of Einstein's equations (45), we get

$$\frac{\dot{a}_0}{\dot{a}_0} = \frac{n'_0}{n_0} \quad (97)$$

Integrating with respect to  $y$ , we get

$$\ln(\dot{a}_0) = \ln(n_0) + \ln(\alpha(\tau))$$

$$\frac{\dot{a}_0}{n_0} = \alpha(\tau) \quad (98)$$

where  $\alpha(\tau)$  is only a function of time. By a suitable change of time, we have

$$n_0 = 1 \quad (99)$$

Then Equation (98) becomes

$$\alpha = \dot{a}_0 \quad (100)$$

Now that we have  $b_0$  and  $n_0$ , to get  $a_0$ , we need to look back at  $F(\tau, y)$  in Equation (46). Since we are only considering a thin spatial slab around  $y = 0$ , we can safely substitute  $b_0 = n_0 = 1$  into Equation (46) and get

$$F(\tau, y) = (a'a)^2 - \alpha^2 a^2 - k a^2 \quad (101)$$

On the other hand, if we set  $\rho_B = 0$ , then the energy-momentum tensor only has the brane

contribution and Equation (48) becomes

$$\begin{aligned}
F' &= -\frac{2a^3a'}{3n^2}\tilde{G}_{00} = -\frac{2a^3a'}{3n^2}\kappa^2(\tilde{T}_{00} + \tilde{U}_{00}) \\
&= -\frac{2a^3a'}{3n^2}\kappa^2(\tilde{T}_0^A\tilde{g}_{A0} + \tilde{U}_{00}) \\
&= -\frac{2a^3a'}{3n^2}\kappa^2\left(\frac{\delta(y)}{b}\rho_b n^2 + \tilde{U}_{00}\right)
\end{aligned} \tag{102}$$

Substitute into  $\tilde{U}_{00}$  from Equation (40), Equation (102) becomes

$$\begin{aligned}
F' &= -\frac{2a^3a'}{3n^2}\kappa^2\left[\frac{\delta(y)}{b}\rho_b n^2 - \frac{3\delta(y)}{\mu^2 b}\left(\frac{\dot{a}^2}{a^2} + k\frac{n^2}{a^2}\right)\right] \\
&= -\frac{2a^3a'}{3n^2}\kappa^2\left[\frac{\delta(y)}{b}\rho_b n^2 - \frac{3\delta(y)}{a^2\mu^2 b}(\dot{a}^2 + kn^2)\right] \\
&= -\frac{2a^3a'\kappa^2\delta(y)}{3b}\rho_b + \frac{2aa'\kappa^2\delta(y)}{n^2\mu^2 b}(\dot{a}^2 + kn^2)
\end{aligned} \tag{103}$$

Again, we can substitute  $b_0 = n_0 = 1$  and  $\alpha = \dot{a}_0$  into the equation and get

$$F' = -\frac{2a^3a'\kappa^2\delta(y)}{3}\rho_b + \frac{2aa'\kappa^2\delta(y)}{\mu^2}(\alpha^2 + k) \tag{104}$$

However, if we differentiate Equation (101) directly, we have

$$F' = 2a'a(a'a)' - 2\alpha^2aa' - 2kaa' \tag{105}$$

We can equate the two equations:

$$\begin{aligned}
2a'a(a'a)' - 2\alpha^2aa' - 2kaa' &= -\frac{2a^3a'\kappa^2\delta(y)}{3}\rho_b + \frac{2aa'\kappa^2\delta(y)}{\mu^2}(\alpha^2 + k) \\
(a'a)' - \alpha^2 - k &= -\frac{a^2\kappa^2\delta(y)}{3}\rho_b + \frac{\kappa^2\delta(y)}{\mu^2}(\alpha^2 + k)
\end{aligned} \tag{106}$$

We integrate the equation in the bulk for  $y > 0$ , then the  $\delta(y)$  terms vanish and we have

$$a'a = (\alpha^2 + k)y + D \tag{107}$$

To calculate the integration constant  $D$ , we evaluate the functions at  $0+$ ,

$$D = a'(0+)a_0 = \frac{1}{2}[a']a_0 \tag{108}$$

and assuming again the  $y$  to  $-y$  symmetry. Now Equation (107) can be written as

$$\frac{1}{2}(a^2)' = (\alpha^2 + k)y + \frac{1}{2}[a']a_0 \quad (109)$$

which integrates to

$$a^2 = (\alpha^2 + k)y^2 + [a']a_0y + E \quad (110)$$

Note that for  $y < 0$ , the integration constant  $D$  takes a different value:

$$D = a'(0-)a_0 = -\frac{1}{2}[a']a_0 \quad (111)$$

Hence the equation in the bulk as a whole is

$$a^2 = (\alpha^2 + k)y^2 + [a']a_0|y| + E \quad (112)$$

Evaluating the function at  $y = 0$ , we get

$$E = a_0^2 \quad (113)$$

Finally, we have  $a^2$  as a quadratic equation of  $y$ :

$$a^2 = (\alpha^2 + k)y^2 + [a']a_0|y| + a_0^2 \quad (114)$$

To fully expand the expression of  $a$  that we have found, we can substitute into the junction condition for  $[a']$  (68):

$$a = a_0 \left\{ 1 + |y| \left[ -\frac{\kappa^2}{3}\rho_b + \frac{\kappa^2}{\mu^2} \left( H^2 + \frac{k}{a_0^2} \right) \right] + y^2 \left( H^2 + \frac{k}{a_0^2} \right) \right\}^{1/2} \quad (115)$$

Substituting into the Friedmann equation (70) for  $C = 0$ , we get

$$a = a_0 \left\{ 1 + 2\epsilon|y| \sqrt{H^2 + \frac{k}{a_0^2}} + y^2 \left( H^2 + \frac{k}{a_0^2} \right) \right\}^{1/2} \quad (116)$$

Since  $y$  is small in the thin slab of universe that we are considering, the equation can be further simplified. We can also get  $n$  using  $n = \frac{\dot{a}}{a_0}$ . Hence the terms of the metric near the



brane are

$$\begin{aligned} a &= a_0 + \epsilon|y|(\dot{a}_0^2 + k)^{1/2} \\ n &= 1 + \epsilon|y|\ddot{a}(\dot{a}_0^2 + k)^{-1/2} \\ b &= 1 \end{aligned} \tag{117}$$

With this, we have found the expression of the variables  $a$ ,  $n$  and  $b$  in the neighborhood of the brane. This is not particularly important in our discussion of the brane cosmology, but it is good to know that the embedding of the brane in the bulk can be done properly.

## 4 Cosmological Solution

### 4.1 Cosmological Solution

After finding the Friedmann equation, we can solve the equation to get a cosmological solution of our universe. In the search of the cosmological solution, we will be restricting the equation to the brane. In the end, we will try to fit the solution to the observation. From here onwards, unless otherwise stated, all the variables are the brane variables. For example,  $a$  denotes the previously used  $a_0$ . We then reuse the subscript 0 in the calculations to denote the current value of the variable, for example,  $a_0$  now denotes the current value of  $a$  instead of the value of  $a$  in the brane.

We begin by rewriting the Friedmann-like equation (70) using the expression of  $r_c$  [12]:

$$\begin{aligned} \epsilon \sqrt{H^2 - \frac{\mu^2 r_c}{3} \rho_B - \frac{C}{a^4} + \frac{k}{a^2}} &= r_c \left[ \left( H^2 + \frac{k}{a^2} \right) - \frac{\mu^2}{3} \rho_b \right] \\ H^2 - \frac{\mu^2 r_c}{3} \rho_B - \frac{C}{a^4} + \frac{k}{a^2} &= r_c^2 \left[ \left( H^2 + \frac{k}{a^2} \right)^2 - \frac{2\mu^2 \rho_b}{3} \left( H^2 + \frac{k}{a^2} \right) + \frac{\mu^4 \rho_b^2}{9} \right] \end{aligned} \quad (118)$$

The equation is simplified to

$$\left( H^2 + \frac{k}{a^2} \right)^2 - \left( \frac{2\mu^2 \rho_b}{3} + \frac{1}{r_c^2} \right) \left( H^2 + \frac{k}{a^2} \right) + \frac{\mu^4 \rho_b^2}{9} + \frac{\mu^2}{3r_c} \rho_B + \frac{C}{a^4 r_c^2} = 0 \quad (119)$$

Then we can solve for  $H^2 + \frac{k}{a^2}$ :

$$H^2 + \frac{k}{a^2} = \frac{\mu^2 \rho_b}{3} + \frac{1}{2r_c^2} \pm \sqrt{\frac{\mu^2 \rho_b}{3r_c^2} + \frac{1}{4r_c^4} - \frac{\mu^2}{3r_c} \rho_B - \frac{C}{a^4 r_c^2}} \quad (120)$$

We can see from the above equation the reappearance of the two branches of solutions and, as always, the lower sign corresponds to *Brane 1* while the upper sign corresponds to *Brane 2*. The first thing to note from the equation is that, as discussed in Section 3.4, we can recover the standard cosmology by assuming  $r_c$  is much larger than  $H^{-1}$ :

$$H^2 + \frac{k}{a^2} = \frac{\mu^2 \rho_b}{3} \quad (121)$$

In this expression, the recovery of the standard cosmology is more apparent and this result

holds for both *Brane 1* and *Brane 2*.

Remember that we also have the usual continuity equation (71) for the fluid densities:

$$\dot{\rho} + 3H(p + \rho) = 0 \quad (122)$$

Thus, we have the usual time evolution for the energy densities, which is given by:

$$\rho = \rho_0(1+z)^{3(1+w)} \quad (123)$$

where  $z$  is the red-shift. If we let the integration constant,  $C$ , be zero, we can then express the Friedmann equation (120) in the following form:

$$\frac{H^2(z)}{H_0^2} = \Omega_k(1+z)^2 + \sum_{\alpha} \Omega_{\alpha}(1+z)^{3(1+w_{\alpha})} + 2\Omega_{r_c} \pm 2\sqrt{\Omega_{r_c}} \sqrt{\sum_{\alpha} \Omega_{\alpha}(1+z)^{3(1+w_{\alpha})} + \Omega_{r_c} + \Omega_B} \quad (124)$$

where we have used the usual density parameters:

$$\begin{aligned} \Omega_k &\equiv -\frac{k}{H_0^2 a_0^2} \\ \Omega_{\alpha} &\equiv \frac{\mu^2 \rho_{\alpha}^0}{3H_0^2 a_0^{3(1+w_{\alpha})}} \\ \Omega_{r_c} &\equiv \frac{1}{4r_c^2 H_0^2} \\ \Omega_B &\equiv -\frac{\kappa^2 \rho_B}{6H_0^2} \end{aligned} \quad (125)$$

Here the  $\rho_{\alpha}$ 's denote cosmic fluids with different equations of state in the brane while  $\rho_B$  is the cosmological constant in the bulk. In this project, we will only be focusing on non-relativistic matter (baryons and dark matter) and cosmological constant in the brane, so  $H$  becomes [6]

$$\frac{H^2(z)}{H_0^2} = \Omega_k(1+z)^2 + \Omega_M(1+z)^3 + \Omega_{\Lambda} + 2\Omega_{r_c} \pm 2\sqrt{\Omega_{r_c}} \sqrt{\Omega_M(1+z)^3 + \Omega_{\Lambda} + \Omega_{r_c} + \Omega_B} \quad (126)$$

This is the expression for Hubble parameter in the DGP model and we will be using this expression extensively in Section 5.

With these equations, we can compare our model with the standard models, whose

conventional equations are:

$$\begin{aligned} H^2(z) &= H_0^2[\Omega_k(1+z)^2 + \Omega_M(1+z)^3 + \Omega_X(1+z)^{3(1+w_X)}] \\ \Omega_k + \Omega_M + \Omega_X &= 1 \end{aligned} \quad (127)$$

where  $\Omega_X$  is a form of dark energy. If the dark energy is the cosmological constant, then the model is reduced to the  $\Lambda$ CDM model. Referring to the standard equations (127), we can see that in the new Hubble parameter (126) the cross-over term plays the role of a cosmological constant, but it also gives rise to an extra non-constant term at the end of the equation, so it will not replace trivially the cosmological constant in the standard model. We see from here the reappearance of the two branches of solution, with the lower and upper sign corresponding to the *Brane 1* and *Brane 2* solutions respectively. It is clear that if  $\Omega_{r_c} = 0$ , then the two solutions merge to become the  $\Lambda$ CDM model, this corresponds to the case  $r_c \rightarrow \infty$ , or equivalently  $\kappa \rightarrow \infty$ , when the 5D term in the action disappears.

In this model, we have one constraint on the parameters which is the normalization condition [6][12]. At  $z = 0$ , Equation (126) becomes

$$1 = \Omega_k + \Omega_M + \Omega_\Lambda + 2\Omega_{r_c} \pm 2\sqrt{\Omega_{r_c}}\sqrt{\Omega_M + \Omega_\Lambda + \Omega_{r_c} + \Omega_B} \quad (128)$$

This put a constraint on the parameters and removes a degree of freedom. In the particular case of a flat universe with no cosmological constant,  $\Omega_k = \Omega_\Lambda = \Omega_B = 0$ , and we have

$$1 = (\sqrt{\Omega_M + \Omega_{r_c}} \pm \sqrt{\Omega_{r_c}})^2 \quad (129)$$

Remember that  $\Omega_{r_c} > 0$  by definition. From observations, we can also assume that  $\Omega_M \geq 0$ . Hence

$$\begin{aligned} 1 &= \sqrt{\Omega_M + \Omega_{r_c}} \pm \sqrt{\Omega_{r_c}} \\ 1 \mp \sqrt{\Omega_{r_c}} &= \sqrt{\Omega_M + \Omega_{r_c}} \\ 1 \mp 2\sqrt{\Omega_{r_c}} + \Omega_{r_c} &= \Omega_M + \Omega_{r_c} \end{aligned} \quad (130)$$

For *Brane 1*, we have

$$\sqrt{\Omega_{r_c}} = \frac{\Omega_M - 1}{2} \quad (131)$$

From the observations,  $\Omega_M$  most likely lies in the range of 0 to 1, so we can immediately see from here that *Brane 1* cannot to be flat without a cosmological constant. On the other

hand, for *Brane 2*, we have

$$\sqrt{\Omega_{r_c}} = \frac{1 - \Omega_M}{2} \quad (132)$$

This equation will be our guideline for a flat universe, in fitting of the parameters, later in Section 5.1.

## 4.2 Luminosity Distance and Angular Diameter Distance

With the Hubble parameter from the model, we can calculate various observable cosmological quantities and compare them with those of the standard cosmology. The first observable quantities calculated are distances.

In cosmology, there are various way of defining a distance; the most basic definition is the comoving distance which does not take into account the expansion of the universe [1]. While the physical distance scales with the scale factor during the expansion, the comoving distance is a physical concept that focuses on other aspects of the cosmology and astrophysics except the expansion. In terms of mathematics, the comoving distance,  $\chi$ , is the distance measured by  $dr/\sqrt{1 - kr^2}$  in the metric (18), while the proper distance is the distance measured by  $adr/\sqrt{1 - kr^2}$ , and the only difference between the distances is the scale factor  $a$ . To simplify the calculations, note that the metric (18) can also be expressed in the following form:

$$ds^2 = -dt^2 + a^2(t)[d\chi^2 + S_k^2(\chi)(d\theta^2 + \sin\theta d\phi^2)] \quad (133)$$

where  $\chi$  is the comoving distance and  $S_k$  is given by:

$$S_k(x) = \begin{cases} \sin x, & k = 1 \\ x, & k = 0 \\ \sinh x, & k = -1 \end{cases} \quad (134)$$

In this form we can see the role of the comoving distance more clearly. Both definitions are equivalent to each other and the comoving distance defined in such a way is  $H_0$  independent and dimensionless.

On the other hand, often associated with the comoving distance is another important distance definition known as the luminosity distance. In cosmological observations, the signals received are various electromagnetic waves, i.e. lights. From this, the cosmologists

derived another definition of distance using the concept of flux of the waves:

$$F = \frac{L_s}{4\pi d^2} \quad (135)$$

where  $F$  is the flux,  $L_s$  is the absolute luminosity of the source of emission and  $d$  is the distance between the emission and the reception. From here, a natural definition of distance, known as the luminosity distance  $d_L$ , is given by [1]:

$$d_L^2 = \frac{L_s}{4\pi F} \quad (136)$$

To find the explicit expression of  $d_L$ , we can consider the situation where an emission was emitted at a source located at  $\chi = \chi_s$  at time  $t = t_1$  and the signal was received at  $\chi = 0$  at  $t = t_0$ . The absolute luminosity of the source is given by the ratio of energy to time:

$$L_s = \frac{\Delta E_1}{\Delta t_1} \quad (137)$$

Remember that energy of a light packet is proportional to its frequency:  $\Delta E_1 \propto \nu_1$ , and the time is inversely proportional to the frequency:  $\Delta t_1 \propto 1/\nu_1$ . So we have:

$$L_s \propto \nu_1^2 \quad (138)$$

Similarly, the luminosity at the reception is given by:

$$L_0 \propto \nu_0^2 \quad (139)$$

Also remember that the wavelength of the light is inversely proportional to the frequency:  $\lambda_1 \propto 1/\nu_1$ ,  $\lambda_0 \propto 1/\nu_0$ . Then the relation between the luminosities is given by:

$$L_s = L_0 \left( \frac{\lambda_0}{\lambda_1} \right)^2 = L_0 (1+z)^2 \quad (140)$$

where we have introduced the red-shift at the end. On the other hand, from the metric (133), we can calculate the area of the sphere at  $t = t_0$  to be  $S = 4\pi[a_0 S_k(\chi)]^2$ . Hence, the observed flux is given by:

$$F = \frac{L_0}{4\pi[a_0 S_k(\chi)]^2} \quad (141)$$

Combining all these terms, the luminosity distance is given by:

$$d_L = a_0 S_k(\chi)(1+z) \quad (142)$$

One first needs to find the comoving distance in order to calculate the luminosity distance. Note that as a consequence of the definition of the comoving distance, the luminosity distance is also  $H_0$  independent and dimensionless.

In order to calculate the comoving distance, remember first that light travels in the special geodesic  $ds^2 = -dt^2 + a^2 d\chi^2 = 0$ . Hence, the comoving distance is given by:

$$\chi = \int_0^{\chi_s} d\chi = \int_{t_1}^{t_0} \frac{dt}{a(t)} \quad (143)$$

In cosmology, it is more convenient to do the integration using the red-shift. From the definition,  $1 + z = a_0/a$ , we can differentiate both sides and get:

$$\dot{z} = -\frac{a_0}{a^2} \dot{a} = -H(1 + z) \quad (144)$$

then we have  $dt = -dz/H(1 + z)$  and the comoving distance can be calculated by:

$$\chi = \int_0^z \frac{dx}{a_0 H(x)} \quad (145)$$

where we have simplified the equation using  $a_0 = a(1 + z)$  and the minus sign is absorbed when we flip the limits.

In our later discussions, in Section 5.4, we will focus on a flat universe. In that case, the luminosity distance is simply given by:

$$d_L = (1 + z) \int_0^z \frac{dx}{H(x)} \quad (146)$$

A plot of luminosity distances for different models is given in Figure 2. From the graph, we can see that with a fixed matter energy density parameter of 0.3, *Brane 1* solution resembles a phantom energy model with  $w < -1$ , *Brane 2* resembles a model with  $-1 < w < 0$ , but they are both expanding faster than a standard cold dark model (SCDM) that is dominated by matter [6]. From the expression of the Hubble parameter (126), we see that for larger  $z$ , we have:

$$H_{SCDM} \leq H_{Brane2} \leq H_{\Lambda CDM} \leq H_{Brane1} \leq H_{dS} \quad (147)$$

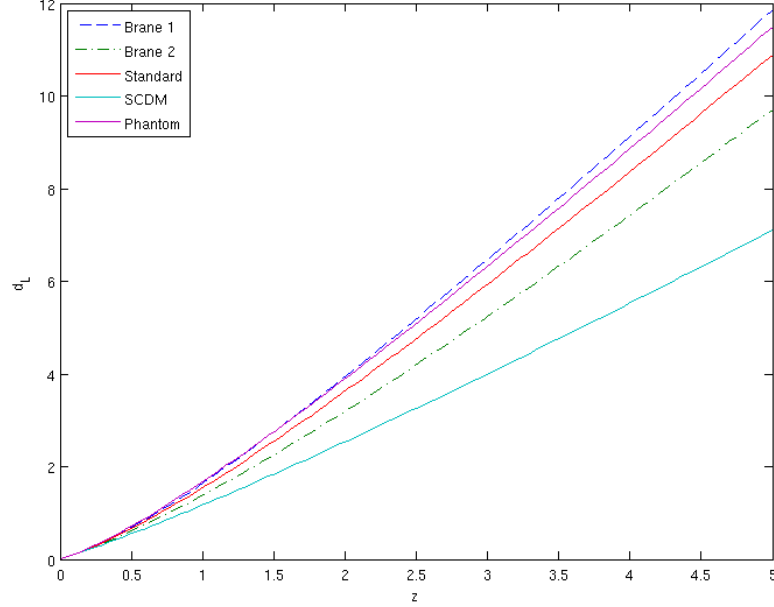


Figure 2: Luminosity distance of different models: *Brane 1* and *Brane 2* are our two branches of solutions, SCDM is the standard cold dark matter model with  $\Omega_M = 1$ ,  $\Lambda$ CDM is the standard model with cosmological constant, and the last one is a model with a dark energy of  $w = -1.5$ . In the models, we assume also a flat universe with no bulk constant:  $\Omega_k = \Omega_B = 0$  and the parameters are  $\Omega_M = 0.3$ ,  $\Omega_{r_c} = 0.3$  for *Brane 1* and *Brane 2*,  $\Omega_\Lambda = 0.7$  for  $\Lambda$ CDM and the phantom energy model.

where the last term is the de Sitter universe. So for luminosity distance, we have:

$$d_L^{SCDM} \leq d_L^{Brane2} \leq d_L^{\Lambda CDM} \leq d_L^{Brane1} \leq d_L^{dS} \quad (148)$$

As for the phantom energy model, it is more irregular: it shows a similar pattern to *Brane 1* for smaller  $z$ ; while for earlier time, i.e. larger  $z$ , *Brane 1* has a larger luminosity distance.

On the other hand, another distance that we can calculate in cosmology is the angular diameter distance, which is  $H_0$  independent [12],

$$d_A = \frac{d_M}{1+z} = \frac{d_L}{(1+z)^2} \quad (149)$$

It is easy to see that the discussions for the luminosity distance are also applicable for the angular diameter distance. A similar plot is given in Figure 3.



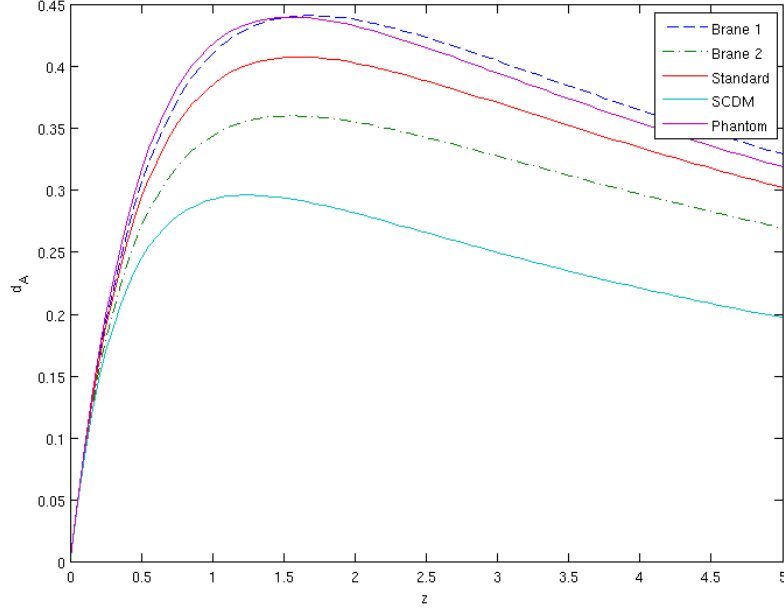


Figure 3: Angular diameter distance of different models: *Brane 1* and *Brane 2* are our two branches of solutions, SCDM is the standard cold dark matter model with  $\Omega_M = 1$ ,  $\Lambda$ CDM is the standard model with cosmological constant, and the last one is a model with a dark energy of  $w = -1.5$ . In the models, we assume also a flat universe:  $\Omega_k = \Omega_B = 0$  and the parameters are  $\Omega_M = 0.3$ ,  $\Omega_{r_c} = 0.3$  for *Brane 1* and *Brane 2*,  $\Omega_\Lambda = 0.7$  for  $\Lambda$ CDM and the phantom energy model.

### 4.3 Deceleration Parameter

Other than comparing the distances, another important parameter to compare is the deceleration parameter,  $q = -\ddot{a}/aH^2$ , which measures the deceleration (acceleration) of the universe. It can be calculated from  $H$  [6]:

$$q(z) = \frac{H'(z)}{H(z)}(1+z) - 1 \quad (150)$$

where the derivation is with respect to  $z$ . Its current value can be calculated by differentiating the Hubble parameter (126) first:

$$\frac{2H(z)H'(z)}{H_0^2} = 2\Omega_k(1+z) + 3\Omega_M(1+z)^2 \pm \sqrt{\Omega_{r_c}} \frac{3\Omega_M(1+z)^2}{\sqrt{\Omega_M(1+z)^3 + \Omega_\Lambda + \Omega_{r_c} + \Omega_B}} \quad (151)$$

If we evaluate the equation (151) at  $z = 0$ , we get:

$$2\frac{H'_0}{H_0} = 2\Omega_k + 3\Omega_M \pm \sqrt{\Omega_{r_c}} \frac{3\Omega_M}{\sqrt{\Omega_M + \Omega_\Lambda + \Omega_{r_c} + \Omega_B}} \quad (152)$$

Hence,  $q_0$  is given by

$$q_0 = \Omega_k + \frac{3\Omega_M}{2} \left( 1 \pm \frac{\sqrt{\Omega_{r_c}}}{\sqrt{\Omega_M + \Omega_\Lambda + \Omega_{r_c} + \Omega_B}} \right) - 1 \quad (153)$$

If we have  $\Omega_k = 0$ , then  $q_0$  is given by

$$q_0 = \frac{3}{2}\Omega_M \left( 1 \pm \sqrt{\frac{\Omega_{r_c}}{\Omega_M + \Omega_\Lambda + \Omega_{r_c} + \Omega_B}} \right) - 1 \quad (154)$$

Hence, a condition to have a flat universe that is currently accelerating is

$$\frac{3}{2}\Omega_M \left( 1 \pm \sqrt{\frac{\Omega_{r_c}}{\Omega_M + \Omega_\Lambda + \Omega_{r_c} + \Omega_B}} \right) < 1 \quad (155)$$

Using the expression of  $H'$  (151), we can plot the full evolution of  $q(z)$  (150), the result is given in Figure 4. We see that with the parameters given, all the models achieve acceleration in current time except the SCDM model. Consistent with previous results, *Brane 1* solution in later time shows a similar behavior to the phantom energy model with an acceleration larger than that of the  $\Lambda$ CDM model; while *Brane 2* solution shows acceleration albeit much smaller than that of the  $\Lambda$ CDM model. From this, we can deduce that to achieve a similar acceleration in current time, our braneworld models require a different setting to the  $\Lambda$ CDM model, and we can boldly proposed that *Brane 1* model needs a larger  $\Omega_M$  to curb the acceleration; while *Brane 2* need a smaller  $\Omega_M$  to enhance the acceleration. We will see this in the result of fitting in Section 5.

#### 4.4 Effective Equation of State

To have a better view of how the *Brane 1* solution resembles a phantom energy model, we can try to define an effective equation of state by comparing our model with the standard model (127). For the standard model,  $H'$  is given by:

$$2H(z)H'(z) = H_0^2[2\Omega_k(1+z) + 3\Omega_M(1+z)^2 + 3(1+w_X)\Omega_X(1+z)^{3(1+w_X)-1}] \quad (156)$$

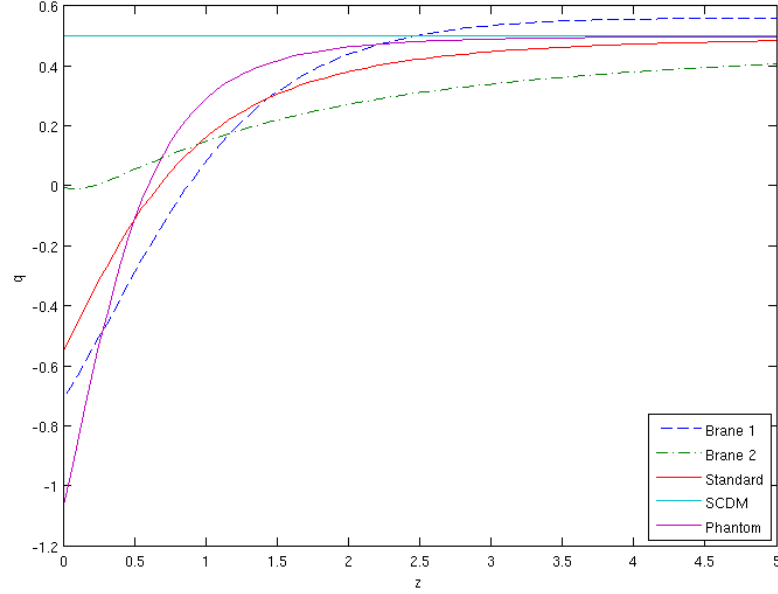


Figure 4: Deceleration parameter,  $q$  of various models: *Brane 1* and *Brane 2* are our two branches of solutions, SCDM is the standard cold dark matter model with  $\Omega_M = 1$ ,  $\Lambda$ CDM is the standard model with cosmological constant, and the last one is a model with a dark energy of  $w = -1.5$ . In the models, we also assume a flat universe:  $\Omega_k = \Omega_B = 0$  and the parameters are  $\Omega_M = 0.3$ ,  $\Omega_{r_c} = 0.3$  for *Brane 1* and *Brane 2*,  $\Omega_\Lambda = 0.7$  for  $\Lambda$ CDM and the phantom energy model.

Then  $q(z)$  is given by:

$$\begin{aligned}
 q(z) &= \frac{2\Omega_k(1+z)^2 + 3\Omega_M(1+z)^3 + 3(1+w_X)\Omega_X(1+z)^{3(1+w_X)}}{\Omega_k(1+z)^2 + \Omega_M(1+z)^3 + \Omega_X(1+z)^{3(1+w_X)}} - 1 \\
 &= \frac{\Omega_k(1+z)^2 + 2\Omega_M(1+z)^3 + (2+3w_X)\Omega_X(1+z)^{3(1+w_X)}}{\Omega_k(1+z)^2 + \Omega_M(1+z)^3 + \Omega_X(1+z)^{3(1+w_X)}}
 \end{aligned} \tag{157}$$

Assuming we have a flat model, i.e.  $\Omega_k = 0$ , then from the normalization condition of the standard model (127) we get:  $\Omega_X = 1 - \Omega_M$ . If we evaluate the equation at  $z = 0$ ,  $q_0$  is given by:

$$q_0 = 2\Omega_M + (2 + 3w_X)(1 - \Omega_M) \tag{158}$$

Finally by rearranging the terms, we get the expression for  $w_X$  in terms of the relative densities:

$$w_X = \frac{2q_0 - 1}{3(1 - \Omega_M)} \tag{159}$$

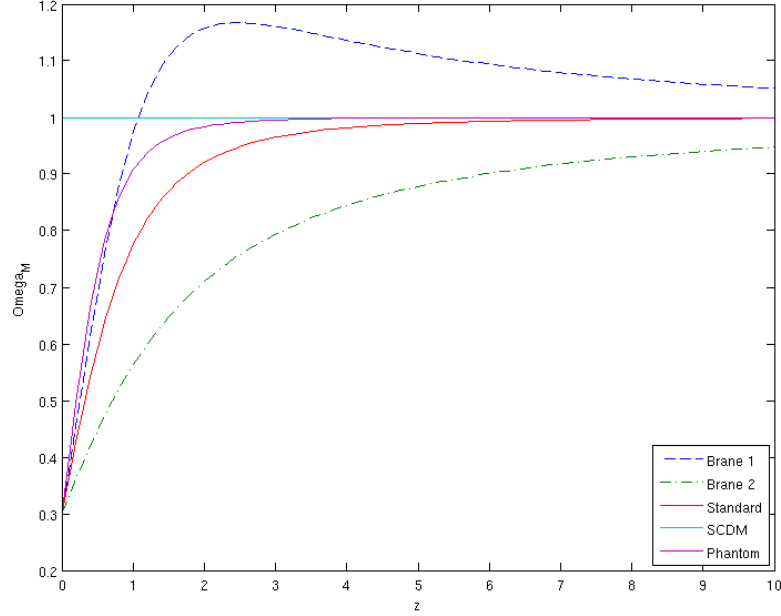


Figure 5: Time-dependent  $\Omega_M$  of various models: *Brane 1* and *Brane 2* are our two branches of solutions, SCDM is the standard cold dark matter model with  $\Omega_M = 1$ ,  $\Lambda$ CDM is the standard model with cosmological constant, and the last one is a model with a dark energy of  $w = -1.5$ . In the models, we also assume a flat universe:  $\Omega_k = \Omega_B = 0$  and the parameters are  $\Omega_M = 0.3$ ,  $\Omega_{r_c} = 0.3$  for *Brane 1* and *Brane 2*,  $\Omega_\Lambda = 0.7$  for  $\Lambda$ CDM and the phantom energy model.

To define a similar quantity for the DGP model to see the evolution of the effective equation of state, we need to define the time-dependant relative density of matter [6]:

$$\Omega_M(z) = \frac{H_0^2}{H^2(z)} \Omega_M(0)(1+z)^3 \quad (160)$$

where  $\Omega_M(0)$  is the parameter  $\Omega_M$  for today. A simple plot of the matter relative density against time for different models is given in Figure 5.

Using the time-dependant  $q(z)$  and  $\Omega_M(z)$ , we can define an effective equation of state for the DGP model in the same form as the usual one [6]:

$$w_{eff}(z) = \frac{2q(z) - 1}{3[1 - \Omega_M(z)]} \quad (161)$$

In particular, if we consider the current value of  $w_{eff}$ :

$$w_{eff}(0) = \frac{2q_0 - 1}{3(1 - \Omega_M)} = -1 \pm \frac{\Omega_M}{1 - \Omega_M} \sqrt{\frac{\Omega_{rc}}{\Omega_M + \Omega_\Lambda + \Omega_{rc} + \Omega_B}} \quad (162)$$

We can clearly see from here that for *Brane 1*, we have  $w_{eff}(0) < -1$  which is similar to a phantom energy; while for *Brane 2*, we have  $-1 < w_{eff}(0) < 0$  which is sandwiched between the  $\Lambda$ CDM and SCDM models.

However, it is important to note that even though *Brane 1* shows a similar behavior to a phantom energy for small  $z$ , they are still different in many ways. For example, we can show that they have a different  $w_{eff}$  in early or late times. If we try to plot  $w_{eff}$  directly, we will encounter a singularity for *Brane 1* at a finite  $z$ . The reason for this singularity lies in the plot of  $\Omega_M(z)$  in Figure 5, we can see that  $\Omega_M(z)$  for *Brane 1* reaches 1 at about  $z = 1$ , so  $w_{eff}$  (161) diverges at this point. However, one should note that this singularity comes from the definition of the effective equation of state, it is not an implicit property of *Brane 1*. This singularity simply means that the definition of this effective equation of state is not suitable for *Brane 1*. Nonetheless, if we scrutinize at the expression of  $w_{eff}$ , assuming  $\Omega_k = 0$ , we see that for late times, when  $z \rightarrow -1$ , for both *Brane 1* and *Brane 2*, we have  $q(z) \rightarrow -1$  and  $\Omega_M(z) \rightarrow 0$ , so  $w_{eff} \rightarrow -1$ . On the other hand for large  $z$ ,  $q(z)$  (150) up to the first order is given by

$$q(z) \approx \frac{1}{2} \mp \frac{3}{2} \sqrt{\frac{\Omega_{rc}}{\Omega_M}} (1 + z)^{-3/2} \quad (163)$$

while  $\Omega_M(z)$  (160) up to the first order is given by

$$\Omega_M(z) \approx 1 \mp 2 \sqrt{\frac{\Omega_{rc}}{\Omega_M}} (1 + z)^{-3/2} \quad (164)$$

So in early times when  $z$  is large, we have  $w_{eff}(z) \rightarrow -0.5$  for both branches again. So *Brane 1* and *Brane 2* share some similar features in the effective equation of state both in early universe and in the future. They are different from a phantom energy which always has  $w < -1$ .

## 5 Fitting of Parameters

### 5.1 Minimum $\chi^2$ Test and Analytic Marginalization

While the qualitative discussions on previous section give a good idea on comparing the DGP model with the standard model in terms of various parameters. To get a more quantitative comparison, we need to do a maximum likelihood test. One of the more popular candidates is the minimum  $\chi^2$  test. The essence of the minimum  $\chi^2$  test is the comparison of an observable quantity calculated from the models to the value observed in experiments assuming a Gaussian error. The probability density function for a parameter  $s$  is given by [13]:

$$\rho(s) \propto \exp\left(-\frac{\chi^2}{2}\right) \quad (165)$$

where  $\chi^2$  is a measure of the difference of the observation from the theoretical value. For a dependant variable  $f$  of parameter  $s$  and independant variable  $t$ ,  $\chi^2$  is given by:

$$\chi^2 = \sum_i \frac{(f(s, t_i) - f_i)^2}{\sigma_i^2} \quad (166)$$

where  $t_i$  is the value of the independant variable in the test and  $\sigma_i$  is the uncertainty. The objective of the test is to find parameter with the maximum probability, and to get the most probable parameters for the model, we have to minimize  $\chi^2$ .

In cosmology, one of the most commonly used observable quantities in minimum  $\chi^2$  test is the luminosity distance, due to the supernovae which act as standard candles in the sky. By knowing the absolute magnitude of the supernovae,  $M$ , the luminosity distance can be calculated by measuring the apparent magnitude,  $m$ :

$$d_L = 10^{(M-m)/5} \quad (167)$$

The difference between the magnitudes is called the distance modulus,  $\mu = M - m$ . To execute the minimum  $\chi^2$  test, it is preferable to calculate the derived variables from the model and compare them directly to the observed quantities. In our case, we are to calculate the theoretical value of  $\mu$  which is given by:

$$\mu(z) = 42.384 + 5 \log \left( \frac{H_0 d_L(z, \Omega_M, \Omega_{r_c})}{c} \right) - 5 \log h \quad (168)$$

Then,  $\chi^2$  is given by

$$\chi^2 = \sum_i \frac{(\mu(z_i) - \mu_0^i)^2}{\sigma_i^2} \quad (169)$$

where  $\mu_0^i$  is the  $i$ -th measured data with uncertainty  $\sigma_i$ . Since  $h$  is independent of the model, we can marginalize over it in the test:

$$\chi_h^2 = -2 \ln \int_0^\infty dh \exp \left( -\frac{\chi^2}{2} \right) \quad (170)$$

In the fitting of the parameters, there is a choice of doing the marginalization of  $h$  numerically [13] or analytically [14]. The numerical marginalization is done by integrating  $\chi_h^2$  numerically; while the analytic marginalization is done by separating  $h$  from the formula and integrate it analytically:

$$\chi^2 = \sum_i \frac{(\mu_*^i - \mu_0^i - 5 \log h)^2}{\sigma_i^2} \quad (171)$$

where  $\mu_*^i = 42.384 + 5 \log(H_0 d_L(z_i)/c)$ . To simplify the calculation, we can define some extra quantities without  $h$ :

$$\begin{aligned} \chi_*^2 &= \sum_i \frac{(\mu_*^i - \mu_0^i)^2}{\sigma_i^2} \\ C_1 &= \sum_i \frac{\mu_*^i - \mu_0^i}{\sigma_i^2} \\ C_2 &= \sum_i \frac{1}{\sigma_i^2} \end{aligned} \quad (172)$$

Then the marginalized  $\chi_h^2$  (170) becomes

$$\chi_h^2 = -2 \ln \int_0^\infty dh \exp \left( -\frac{\chi_*^2}{2} + 5C_1 \log h - \frac{25}{2} C_2 (\log h)^2 \right) \quad (173)$$

If we do a change of variable:  $u = \ln h$ , we get

$$\begin{aligned}
\chi_h^2 &= -2 \ln \int_{-\infty}^{\infty} du e^u \exp \left( -\frac{\chi_*^2}{2} + \frac{5C_1}{\ln 10} u - \frac{25C_2}{2(\ln 10)^2} u^2 \right) \\
&= -2 \ln \int_{-\infty}^{\infty} du \exp \left[ -\frac{\chi_*^2}{2} + \left( \frac{5C_1}{\ln 10} + 1 \right) u - \frac{25C_2}{2(\ln 10)^2} u^2 \right] \\
&= -2 \ln \int_{-\infty}^{\infty} du \exp \left[ -\frac{1}{2} \left( \frac{5\sqrt{C_2}}{\ln 10} u - \frac{5C_1 + \ln 10}{5\sqrt{C_2}} \right)^2 + \frac{1}{2} \left( \frac{5C_1 + \ln 10}{5\sqrt{C_2}} \right)^2 - \frac{\chi_*^2}{2} \right] \\
&= -2 \ln \left[ \sqrt{2\pi} \frac{\ln 10}{5\sqrt{C_2}} \exp \left( \frac{1}{2} \left( \frac{5C_1 + \ln 10}{5\sqrt{C_2}} \right)^2 - \frac{\chi_*^2}{2} \right) \right] \\
&= \ln \left( \frac{25C_2}{2\pi(\ln 10)^2} \right) - \left( \frac{5C_1 + \ln 10}{5\sqrt{C_2}} \right)^2 + \chi_*^2 \\
&= \chi_*^2 - \frac{1}{C_2} \left( C_1 + \frac{\ln 10}{5} \right)^2 + \ln \left( \frac{25C_2}{2\pi(\ln 10)^2} \right)
\end{aligned}$$

Instead of integrating over  $h$ , we calculate  $\chi_*^2$ ,  $C_1$ ,  $C_2$  using the formula given in Equation (172) and substitute them into  $\chi_h^2$ :

$$\chi_h^2 = \chi_*^2 - \frac{C_1}{C_2} \left( C_1 + \frac{2 \ln 10}{5} \right) + \ln \left( \frac{25C_2}{2\pi(\ln 10)^2} \right) - \frac{(\ln 10)^2}{25C_2} \quad (174)$$

In a paper by Yun Wang *et al.* [14], they proposed a modified  $\chi^2$  method. Their definitions for the terms  $\chi_*^2$ ,  $C_1$  and  $C_2$  are essentially same as ours, except that they include an artificial  $h_*$  term in  $\mu_*^i$ :

$$\mu_*^i = 42.384 + 5 \log(H_0 d_L(z_i)/c) - 5 \log h_*$$

To avoid any dependance on the newly introduced  $h_*$ , they have added an extra term in their modified  $\tilde{\chi}^2$ :

$$\tilde{\chi}^2 = \chi_*^2 - \frac{C_1}{C_2} \left( C_1 + \frac{2 \ln 10}{5} \right) - 2 \ln h_*$$

This doesn't affect the best-fit of the model because the extra constants ( $C_2$  and  $h_*$ ) are parameter-independent.

Since the uncertainties of the samples are independant of  $h$ , all methods described above should give the same result. To experiment, all three methods: the numerically marginalized  $\chi^2$  test, the modified  $\chi^2$  test and the analytically marginalized  $\chi^2$  test are carried out and compared. We started with the less exotic model: the *Brane 2* model,



	$\Omega_M$	$\Omega_{r_c}$	Minimum $\chi^2$
$\chi^2$ test	0.335	0.242	180.08
Modified $\chi^2$ test	0.335	0.241	176.00
Analytic $\chi^2$ test	0.335	0.241	183.75

Table 1: The best-fit of three different methods of marginalization of  $h$ .

which is the solution that has been studied extensively in the paper of Deffayet [12]. In the first fitting, the constraint of a flat universe is relaxed and we tried to fit the model without cosmological constants, so the parameters involved are  $\Omega_M$ ,  $\Omega_{r_c}$  and  $h$ . The parameters are fitted with the 156 gold samples from Riess *et al.* (2004) [15] and the result is shown in Table 1 and the contours are plotted in Figure 6. All contours closely resemble each other and that confirms the equivalence of numerical and analytical marginalizations over  $h$ . This gives us a freedom to choose the method to marginalize the  $\chi^2$ . In terms of the amount of computational time needed, the modified  $\chi^2$  test and the analytic  $\chi^2$  test are about the same; but since the analytic  $\chi^2$  test is an original calculation done by me, we choose to use it for our subsequent fittings.

Inspired by the work of Fairbairn and Goobar [17], the parameters were also fitted using the prior from the baryon acoustic oscillation peak detected in the SDSS Luminous Red Galaxy survey (LRG) of Eisenstein *et al.* (2005) [18], given by

$$\frac{\sqrt{\Omega_M}}{E(z_1)^{\frac{1}{3}}} \left[ \frac{1}{z_1 \sqrt{|\Omega_k|}} S \left( \sqrt{|\Omega_k|} \int_0^{z_1} \frac{dz}{E(z)} \right) \right]^{\frac{2}{3}} = 0.469 \pm 0.017, \quad (175)$$

where  $E(z) = H(z)/H_0$  and  $z_1 = 0.35$ . The result is compared to the result of SN1a and presented in Figure 7. With our larger sample group, we are able to reproduce a similar result to the original paper but with a better resolution, and the fitting result seems unfavorable to our DGP model. The model with no cosmological constant is unlikely to be a flat universe. With the BAO prior, the overlapping region is situated well off the line of  $\Omega_k = 0$ . This is undesirable, but we will move on and repeat the test using a more up-to-date data to confirm the result.

The more recent data with which we have chosen to test our model is the latest SN1a data from the Supernova Legacy Survey [19]. In the survey, the observations are made on the apparent magnitude of the supernovae. In this case,  $\chi^2$  is given by

$$\chi^2 = \sum_i \frac{(m_B^i - m_{B;mod}^i)^2}{\sigma_i^2} \quad (176)$$

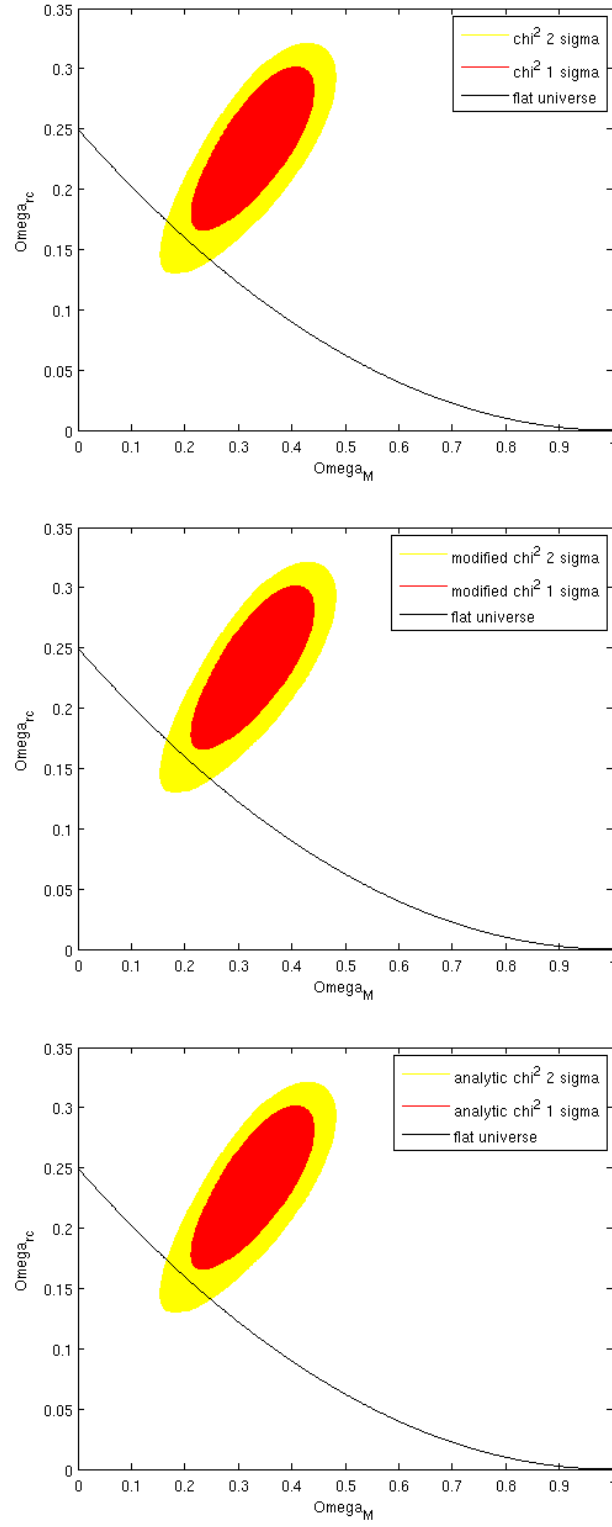


Figure 6: (a) The  $\chi^2$  is calculated by marginalizing over  $h$  numerically, (b) by the modified  $\chi^2$  test, and (c) by the analytic marginalization.  $\Omega_k = 0$  is shown as a curve in each plot.

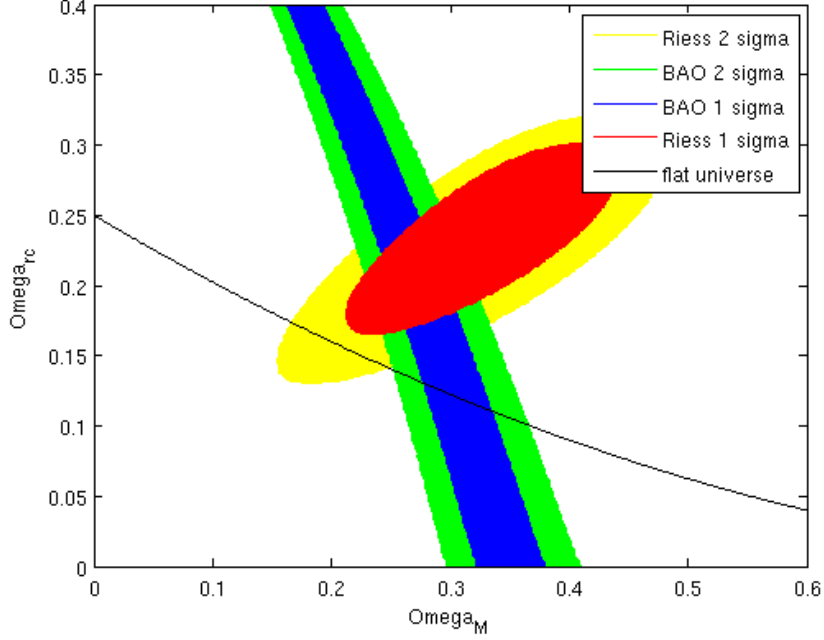


Figure 7: The fitting result of SN1a (Riess 2004) with the prior from BAO (Eisenstein 2005). The line is the constraint of requiring  $\Omega_k = 0$ .

where  $m_B$  is the measured rest-frame peak B-band magnitude of a supernova,  $m_{B;mod}$  is the predicted magnitude given by the model with corrections from two other quantities (stretch,  $s$ , and color,  $C$ ) measured from the light curve, and  $\sigma$  is the total uncertainties from all measured quantities. The predicted magnitude is given by

$$m_{B;mod} = 5 \log \left( \frac{H_0 d_L}{c} \right) + 42.384 - 5 \log h + M - \alpha(s - 1) + \beta C \quad (177)$$

Similarly, since the uncertainties of the samples are independent of  $M$ , we have the option to do the marginalization analytically using a flat prior [20].

$$\chi_M^2 = -2 \ln \int_{-\infty}^{\infty} dM \exp \left( -\frac{\chi^2}{2} \right) \quad (178)$$

We can do a similar calculation by defining

$$\begin{aligned}\tilde{\chi}_*^2 &= \sum_i \frac{(m_B^i - m_*^i)^2}{\sigma_i^2} \\ \tilde{C}_1 &= \sum_i \frac{m_B^i - m_*^i}{\sigma_i^2} \\ \tilde{C}_2 &= \sum_i \frac{1}{\sigma_i^2}\end{aligned}\tag{179}$$

where  $m_*^i = 5 \log \left( \frac{H_0 d_L}{c} \right) + 42.384 - 5 \log h - \alpha(s-1) + \beta C$ . Then the marginalized  $\chi_M^2$  (178) becomes

$$\begin{aligned}\chi_M^2 &= -2 \ln \int_{-\infty}^{\infty} dM \exp \left( -\frac{\tilde{\chi}_*^2}{2} + \tilde{C}_1 M - \frac{1}{2} \tilde{C}_2 M^2 \right) \\ &= -2 \ln \int_{-\infty}^{\infty} dM \exp \left( -\frac{1}{2} \left( M \sqrt{\tilde{C}_2} - \frac{\tilde{C}_1}{\sqrt{\tilde{C}_2}} \right)^2 + \frac{\tilde{C}_1^2}{2\tilde{C}_2} - \frac{\tilde{\chi}_*^2}{2} \right) \\ &= -2 \ln \left( \frac{\sqrt{2\pi}}{\sqrt{\tilde{C}_2}} \exp \left( \frac{\tilde{C}_1^2}{2\tilde{C}_2} - \frac{\tilde{\chi}_*^2}{2} \right) \right) \\ &= \ln \frac{\tilde{C}_2}{2\pi} - \frac{\tilde{C}_1^2}{\tilde{C}_2} + \tilde{\chi}_*^2\end{aligned}$$

So the marginalized  $\chi_M^2$  is given by

$$\chi_M^2 = \tilde{\chi}_*^2 - \frac{\tilde{C}_1^2}{\tilde{C}_2} + \ln \frac{\tilde{C}_2}{2\pi}\tag{180}$$

However, in this case, there is the question of whether one can do the analytic marginalization of  $h$  and  $M$  at the same time. We attempted to do so by using a new variable  $u = M + 5 \log h$ . In this case, the end result will be similar to the analytic marginalization of  $M$ :

$$\chi_{M,h}^2 = \tilde{\chi}_*^2 - \frac{\tilde{C}_1^2}{\tilde{C}_2} + \ln \frac{\tilde{C}_2}{2\pi}\tag{181}$$

where the definition of  $\tilde{\chi}^2$ ,  $\tilde{C}_1$  and  $\tilde{C}_2$  are the same but with a  $h$ -free  $m_*^i$ :  $m_*^i = 5 \log \left( \frac{H_0 d_L}{c} \right) + 42.384 - \alpha(s-1) + \beta C$ . The idea is tested experimentally using the 472 supernovae samples of SNLS and the result is given in Table 2 and the contours are plotted in Figure 8. All the different methods give the same best-fit of  $\Omega_M$  and  $\Omega_{rc}$ , the difference in  $\chi^2$  is only due to the difference in definition. This result verifies that we can indeed do the marginalization

	$\Omega_M$	$\Omega_{r_c}$	$\chi^2$
$\chi^2$ test	0.21	0.23	299.5988
Modified $\chi^2$ test	0.21 (0.203)	0.23 (0.226)	312.6416 (293.9653)
Analytic $\chi^2$ test	0.21	0.23	303.2513
Analytic $\chi^2$ test 2	0.21	0.23	301.0285
Analytic $\chi^2$ test 3	0.21 (0.203)	0.23 (0.226)	301.0285 (301.0120)

Table 2: The best-fits of different methods of marginalization: (a) Numerical marginalization; (b) Modified  $\chi^2$  test; (c) Analytic marginalization over  $h$  only; (d) Analytic marginalization over  $M$  only; (e) Analytic marginalization over  $M$  and  $h$  at the same time. Note that the modified  $\chi^2$  test and type 3 analytic  $\chi^2$  test is repeated with smaller steps and the result is given in parentheses.

of  $M$  and  $h$  at the same time. Hence forth, all the fitting using the gold samples of Riess will be done using the analytic  $\chi^2$  test; while the fitting using the SNLS data will be done using type 3 analytic  $\chi^2$  test which is to marginalize analytically  $M$  and  $h$  at the same time.

For comparison, the plot of SN1a data with BAO prior was updated using the new SNLS data and the result is given in Figure 9. The plot verifies again the result of Fairbaine and Goobar that the best-fit of the DGP model with no cosmological constant is not flat. This result will be examined further, together with other cases of the DGP model in Section 5.3.

## 5.2 Normalization Condition

After establishing a working method to minimize the  $\chi^2$ , we can now do the fitting of parameters under various assumptions. Before we proceed with the fitting, let's reconsider the normalization condition (128):

$$\begin{aligned}
 1 &= \Omega_k - \Omega_B + (\sqrt{\Omega_M + \Omega_\Lambda + \Omega_{r_c} + \Omega_B} \pm \sqrt{\Omega_{r_c}})^2 \\
 1 - \Omega_k + \Omega_B &= (\sqrt{\Omega_M + \Omega_\Lambda + \Omega_{r_c} + \Omega_B} \pm \sqrt{\Omega_{r_c}})^2
 \end{aligned} \tag{182}$$

Here we see an implicit constraint:  $1 - \Omega_k + \Omega_B \geq 0$ . Depending on the sign of  $\Omega_M + \Omega_\Lambda + \Omega_B$ , Equation (182) can have two different outcomes [6].

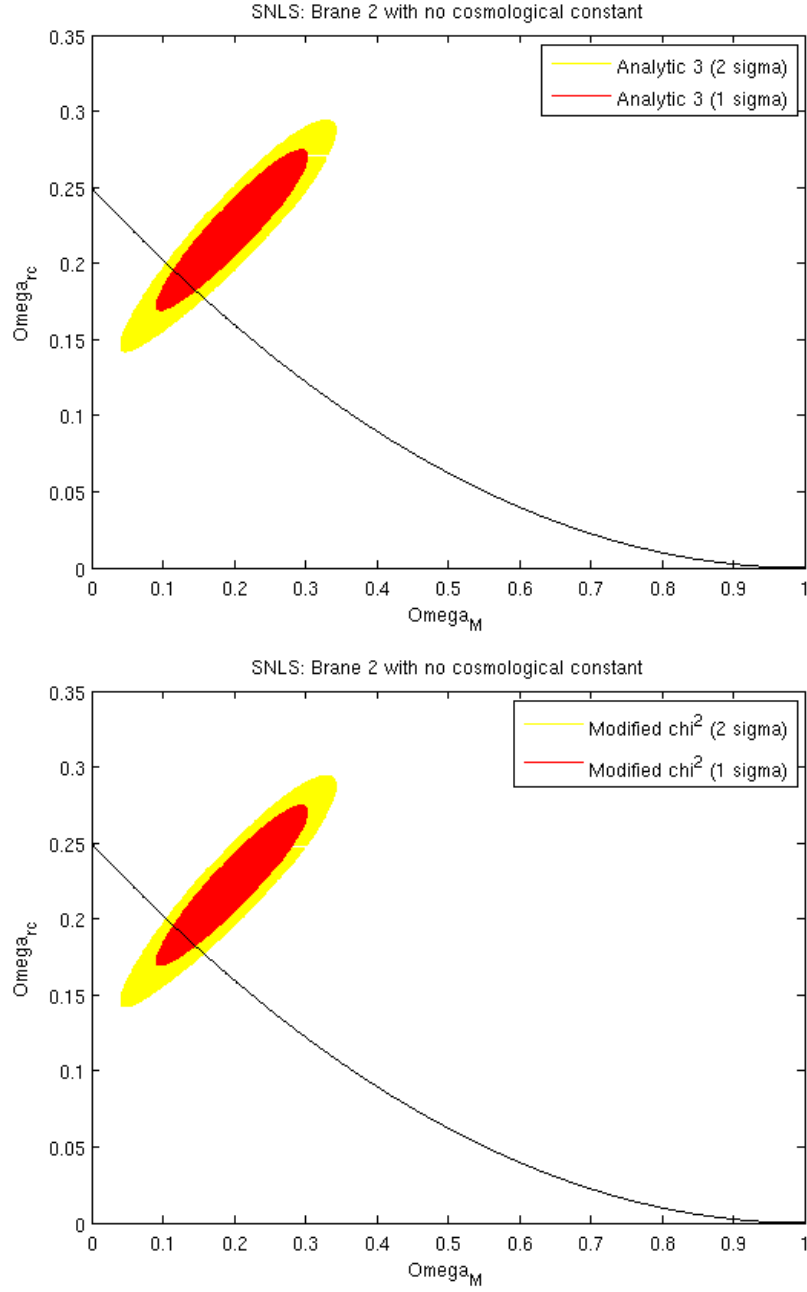


Figure 8: The fitting results of SNLS data with different marginalizations: (a) The analytic marginalization as described in Equation (181); (b) the modified  $\chi^2$  test. The line is the constraint of requiring  $\Omega_k = 0$ .

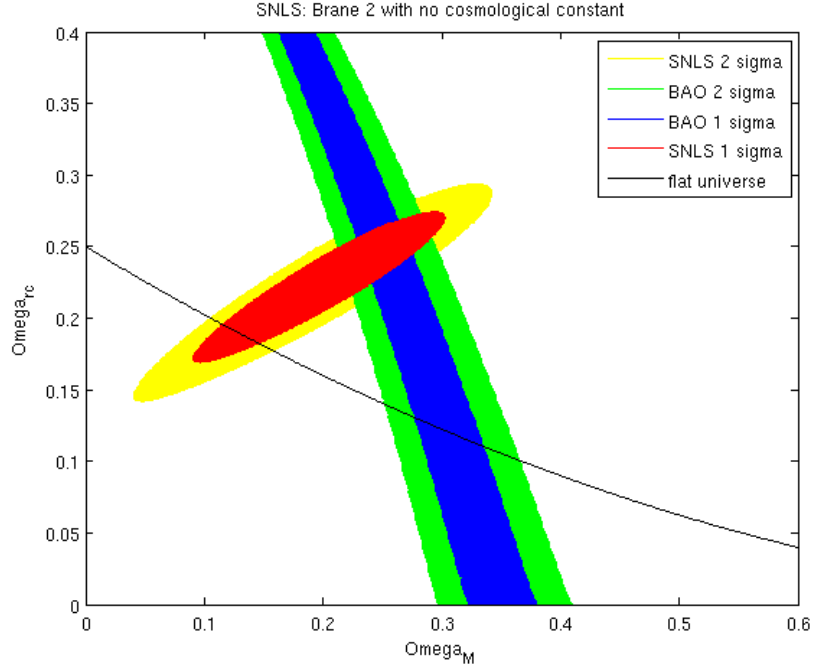


Figure 9: The SNLS data fitted using type 3 analytic marginalization with a prior from BAO. The line is the constraint of requiring  $\Omega_k = 0$ .

If  $\Omega_M + \Omega_\Lambda + \Omega_B < 0$ , we have

$$\begin{aligned}
 \sqrt{1 - \Omega_k + \Omega_B} &= \sqrt{\Omega_{r_c}} - \sqrt{\Omega_M + \Omega_\Lambda + \Omega_{r_c} + \Omega_B} \\
 \sqrt{\Omega_{r_c}} - \sqrt{1 - \Omega_k + \Omega_B} &= \sqrt{\Omega_M + \Omega_\Lambda + \Omega_{r_c} + \Omega_B} \\
 1 - \Omega_k + \Omega_B + \Omega_{r_c} - 2\sqrt{\Omega_{r_c}}\sqrt{1 - \Omega_k + \Omega_B} &= \Omega_M + \Omega_\Lambda + \Omega_{r_c} + \Omega_B
 \end{aligned}$$

Note that in this case, we have another implicit constraint:  $\Omega_{r_c} \leq 1 - \Omega_k + \Omega_B$ , and the normalization condition (128) becomes

$$\Omega_k + \Omega_M + \Omega_\Lambda + 2\sqrt{\Omega_{r_c}}\sqrt{1 - \Omega_k + \Omega_B} = 1 \quad (183)$$

for both *Brane 1* and *Brane 2*. However, it is not hard to see that *Brane 1* with the new normalization condition (183) has a Hubble parameter that reaches zero for a finite  $z$ . For simplicity, we will not consider *Brane 1* with these parameters.

On the other hand if  $\Omega_M + \Omega_\Lambda + \Omega_B \geq 0$ , Equation (182) becomes

$$\begin{aligned}\sqrt{1 - \Omega_k + \Omega_B} &= \sqrt{\Omega_M + \Omega_\Lambda + \Omega_{r_c} + \Omega_B} \pm \sqrt{\Omega_{r_c}} \\ \sqrt{1 - \Omega_k + \Omega_B} \mp \sqrt{\Omega_{r_c}} &= \sqrt{\Omega_M + \Omega_\Lambda + \Omega_{r_c} + \Omega_B} \\ 1 - \Omega_k + \Omega_B + \Omega_{r_c} \mp 2\sqrt{\Omega_{r_c}}\sqrt{1 - \Omega_k + \Omega_B} &= \Omega_M + \Omega_\Lambda + \Omega_{r_c} + \Omega_B\end{aligned}$$

So the normalization condition (128) becomes

$$\Omega_k + \Omega_M + \Omega_\Lambda \pm 2\sqrt{\Omega_{r_c}}\sqrt{1 - \Omega_k + \Omega_B} = 1 \quad (184)$$

where again the lower and upper sign corresponds to *Brane 1* and *Brane 2* respectively. We see that *Brane 2* always has the same normalization condition (183). On the other hand for *Brane 1*, with the new normalization condition (184), we have

$$\begin{aligned}\Omega_M + \Omega_\Lambda + \Omega_B &= 1 - \Omega_k + \Omega_B + 2\sqrt{\Omega_{r_c}}\sqrt{1 - \Omega_k + \Omega_B} \\ &= \sqrt{1 - \Omega_k + \Omega_B}(\sqrt{1 - \Omega_k + \Omega_B} + 2\sqrt{\Omega_{r_c}}) \\ &\geq 0\end{aligned}$$

So the condition  $\Omega_M + \Omega_\Lambda + \Omega_B \geq 0$  is self-satisfied.

In conclusion, we can always use normalization condition (184) for the fitting of *Brane 1* and *Brane 2*. Remember that we also have an implicit condition:  $1 - \Omega_k + \Omega_B \geq 0$  for *Brane 1* and  $1 - \Omega_k + \Omega_B \geq \Omega_{r_c}$  for *Brane 2*.

### 5.3 Fitting Results: DGP Model with No Cosmological Constant

To begin our fitting of parameters, we should first revisit *Brane 2* in the same setting as in the previous section: no cosmological constant, but the flatness of the universe is relaxed. The result is presented in Table 3. Based on current observations, our universe is likely to be a flat one. So, we also fitted the data with  $\Omega_k$  fixed to 0 and the normalization condition (132). The result is given in Table 4. Remember that it is not possible for *Brane 1* to be flat without a cosmological constant. In particular, we also calculated the  $\chi^2$  by fixing the relative matter density  $\Omega_M = 0.3$  and  $\Omega_{r_c} = 0.1225$  to model a flat universe with no cosmological constant. The result is given in Table 5.

For comparison, we also calculated the best-fit of the  $\Lambda$ CDM model. From the expression of  $H$  (126), this is done simply by setting  $\Omega_{r_c} = 0$ . The result is presented in Table 6. We



also calculated the  $\chi^2$  for  $\Omega_M = 0.3$  and the result is given in Table 7. We can see from the table that our model without a cosmological constant is still not as good as the  $\Lambda$ CDM model in terms of  $\chi^2$ . From there, we have to include cosmological constants in our next fitting.

#### 5.4 Fitting Results: DGP Model with Brane and Bulk Cosmological Constants

From this point onwards, based on the result of the CMB observation, we will be focusing on flat universes with cosmological constants by setting  $\Omega_k = 0$ . If we look at the normalization condition for *Brane 1*, it is now simplified to:

$$\Omega_M + \Omega_\Lambda - 2\sqrt{\Omega_{r_c}}\sqrt{1 + \Omega_B} = 1 \quad (185)$$

and we have to ensure that  $1 + \Omega_B \geq 0$ . In this fitting, as before, we will be using  $\Omega_M$  and  $\Omega_{r_c}$  as independent parameters together with a new independent parameter  $\Omega_B$ .  $\Omega_\Lambda$  on the other hand will be constrained by the normalization condition. Compare to the previous fittings, we have relaxed the constraints by allowing both brane and bulk cosmological constants to be non-zero. For simplicity, we only test the models using the more up-to-date data set which is the SNLS data. The result is given in Table 8.

In comparison with *Brane 1*, we can repeat the same setting in the fitting of *Brane 2* with the normalization condition (184):

$$\Omega_M + \Omega_\Lambda + 2\sqrt{\Omega_{r_c}}\sqrt{1 + \Omega_B} = 1 \quad (186)$$

The condition to be ensured is  $\Omega_{r_c} \leq 1 + \Omega_B$ . The result of fitting is also given in Table 8.

In Table 8, we can see that we have  $\Omega_{r_c} = 0$  in our best-fit for *Brane 2*, which means that the model is reverted back to a standard  $\Lambda$ CDM model. However, the difference in  $\chi^2$  suggests that under similar circumstances, *Brane 1* fits slightly better than the  $\Lambda$ CDM model.

Even so, the value of  $\Omega_M$  in the best-fit of *Brane 2* or the  $\Lambda$ CDM model deviates too much from the expected  $\Omega_M \approx 0.3$ . In view of that, the fitting is repeated by setting  $\Omega_M = 0.3$ . In this fitting, we can plot the contour for the 2 independent parameters, however it is more interesting to compare the dynamic between the brane cosmological constant and

Model	Data Set	$\Omega_M$	$\Omega_{r_c}$	$\Omega_k$	$\chi^2$
<i>Brane 2</i>	Riess	0.335	0.241	-0.5622	183.7514
	SNLS	0.203	0.226	-0.278	301.0120

Table 3: The fitting result of *Brane 2* using Riess and SNLS data with no cosmological constant:  $\Omega_\Lambda = \Omega_B = 0$ , but the constraint of flat universe is relaxed and we have  $\Omega_k = 1 - \Omega_M - 2\Omega_{r_c} - 2\sqrt{\Omega_{r_c}}\sqrt{\Omega_M + \Omega_{r_c}}$ .

Model	Data Set	$\Omega_M$	$\Omega_{r_c}$	$\chi^2$
<i>Brane 2</i>	Riess	0.204	0.158	186.7053
	SNLS	0.130	0.189	302.0360

Table 4: The fitting result of a flat *Brane 2* with no cosmological constant:  $\Omega_k = \Omega_\Lambda = \Omega_B = 0$ .

Model	Data Set	$\Omega_M$	$\Omega_{r_c}$	$\chi^2$
<i>Brane 2</i>	Riess	0.3	0.123	193.7981
	SNLS	0.3	0.123	387.0103

Table 5:  $\chi^2$  of a flat *Brane 2* with  $\Omega_M = 0.3$  and no cosmological constant:  $\Omega_k = \Omega_\Lambda = \Omega_B = 0$ .

Model	Data Set	$\Omega_M$	$\Omega_\Lambda$	$\chi^2$
$\Lambda$ CDM	Riess	0.308	0.692	185.6981
	SNLS	0.214	0.786	301.5454

Table 6: The fitting result of the  $\Lambda$ CDM model, i.e.  $\Omega_{r_c} = 0$ .

Model	Data Set	$\Omega_M$	$\Omega_\Lambda$	$\chi^2$
$\Lambda$ CDM	Riess	0.3	0.7	185.7467
	SNLS	0.3	0.7	318.3544

Table 7:  $\chi^2$  of the  $\Lambda$ CDM model, i.e.  $\Omega_{r_c} = 0$ , with  $\Omega_M = 0.3$ .

Model	Data Set	$\Omega_M$	$\Omega_{r_c}$	$\Omega_B$	$\Omega_\Lambda$	$\chi^2$
<i>Brane 1</i>	SNLS	0.28	0.01	-1.00	0.72	300.3795
<i>Brane 2</i>	SNLS	0.21	0	-1.00	0.79	301.5828

Table 8: Best-fit of *Brane 1* and *Brane 2* assuming a flat universe.

the bulk constant, so we choose to use them as independent parameters instead. In this case,  $\Omega_{r_c}$  is calculated from the normalization condition using  $\Omega_\Lambda$  and  $\Omega_B$ . For *Brane 1*, the normalization condition becomes:

$$\begin{aligned}\Omega_\Lambda - 2\sqrt{\Omega_{r_c}}\sqrt{1 + \Omega_B} &= 0.7 \\ \Omega_{r_c} &= \frac{(\Omega_\Lambda - 0.7)^2}{4(1 + \Omega_B)}\end{aligned}\tag{187}$$

As always, we have the implicit constraint:  $1 + \Omega_B \geq 0$ , but now we have a new constraint:  $\Omega_\Lambda \geq 0.7$ . Note that when  $\Omega_\Lambda = 0.7$  and  $\Omega_B = -1$ ,  $\Omega_{r_c}$  is degenerated and can take on any value. With these constraints, the fitting is carried out and the result is given in Table 9, the corresponding contours are given in Figure 10.

On the other hand for *Brane 2*, we have the following new normalization condition:

$$\begin{aligned}\Omega_\Lambda + 2\sqrt{\Omega_{r_c}}\sqrt{1 + \Omega_B} &= 0.7 \\ \Omega_{r_c} &= \frac{(0.7 - \Omega_\Lambda)^2}{4(1 + \Omega_B)}\end{aligned}\tag{188}$$

The condition to check for *Brane 2* is  $\Omega_{r_c} \leq 1 + \Omega_B$  or equivalently  $\Omega_\Lambda \geq 0.7 - 2(1 + \Omega_B)$ . On the other hand, we can see from the equation that we also have  $\Omega_\Lambda \leq 0.7$ , i.e. we have  $0.7 - 2(1 + \Omega_B) \leq \Omega_\Lambda \leq 0.7$ . Note that like in the case of *Brane 1*,  $\Omega_{r_c}$  appears to be degenerated when  $\Omega_\Lambda = 0.7$  and  $\Omega_B = -1$ , however if we go back to Equation (128), we see that  $\Omega_{r_c}$  is actually forced to take on the value 0, so there is no degeneracy here. With the constraint on the range of  $\Omega_\Lambda$ , the fitting is carried out and the result is summarized in Table 9 and the contours are given in Figure 10.

From the result of Table 9, we can see again that *Brane 1* fits noticeably better than *Brane 2* which again has the  $\Lambda$ CDM model as the best-fit. Although this comes at a cost of using the brane cosmological constant of the standard value ( $\Omega_\Lambda = 0.7$ ) and hence doesn't solve the cosmological constant problem, this is still an interesting discovery. Another interesting feature of the model that one cannot directly see from Table 8 and Table 9 is the insensitivity of the bulk cosmological constant  $\Omega_B$  as a parameter. We can see that in the expression of  $H$  (126),  $\Omega_B$  plays a noticeably smaller role than the others because it only appears in a square-root term, hence a larger variation of the parameter is required to affect the result of the fitting.

To have a better feel of the roles of the brane and bulk constants, the general case above can also be split into two cases, where in each case we allow only a brane or a bulk

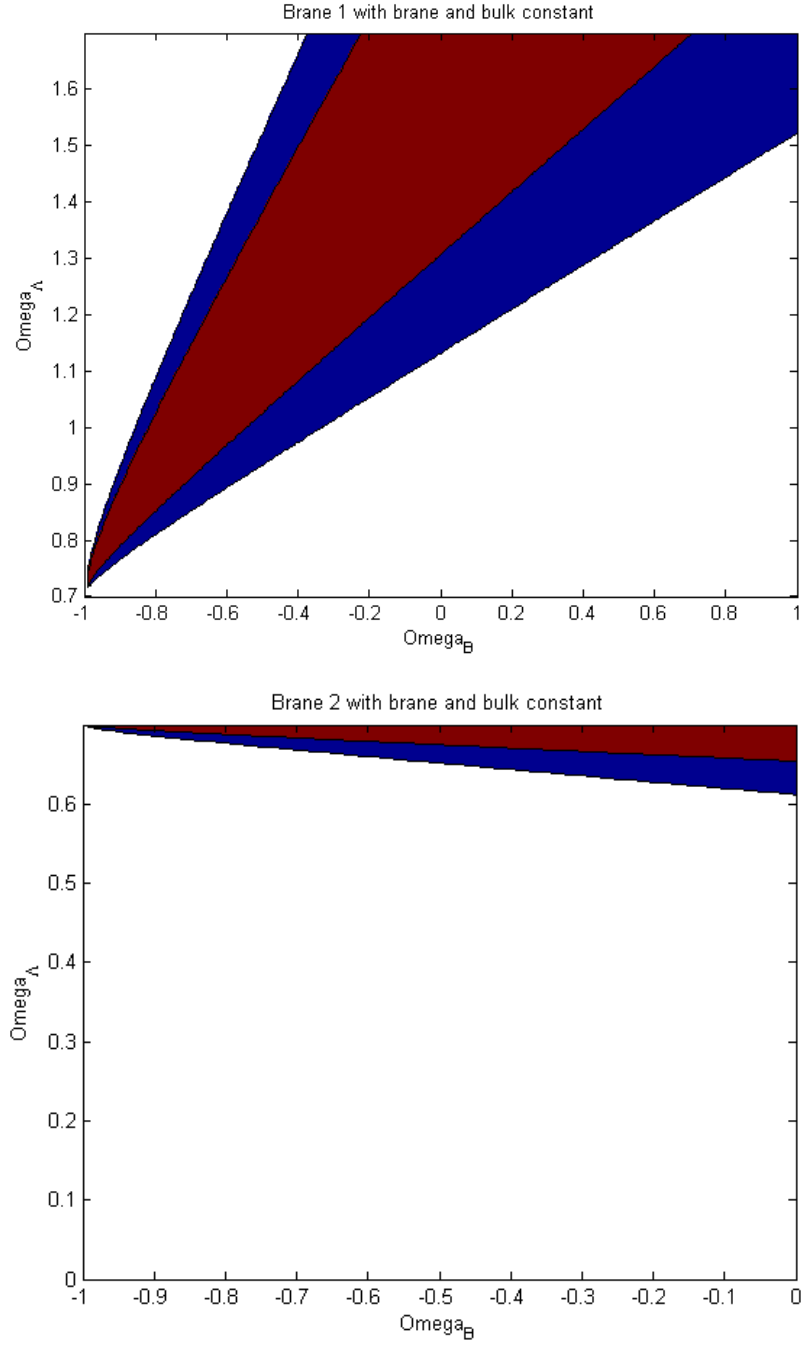


Figure 10: *Brane 1* and *Brane 2* with brane and bulk constant,  $\Omega_M = 0.3$ .

constant. Note that for the case of only the bulk constant, the normalization condition (184) for *Brane 1* becomes:

$$\Omega_M = 1 + 2\sqrt{\Omega_{r_c}}\sqrt{1 + \Omega_B} \quad (189)$$

and we are back to the unrealistic situation that  $\Omega_M \geq 1$ . Hence, the case of DGP model with only the bulk constant is not considered here. The result for the cases with only the brane constant is given in Table 10; while the fitting result for *Brane 2* with only the bulk constant is given in Table 12. As we can see, the difference in  $\chi^2$  for the best-fit under different circumstances is little, so the fitting cannot distinguish the models. The corresponding contours are given in Figure 11. For reference, the fitting for fixed  $\Omega_M = 0.3$  is also presented in Table 11 and Table 13.

In conclusion, the fitting of the DGP model assuming a flat universe with no cosmological constant is no better than the  $\Lambda$ CDM model. That said, the difference in  $\chi^2$  for the best-fit of different models is indistinguishable, so we cannot reach a definitive conclusion. The idea of accelerating expansion with no cosmological constant is certainly interesting as it will lift entirely the problem of the cosmological problem, but the result of the minimum  $\chi^2$  test suggests that it is less likely the case. On the other hand, if we allow brane and bulk cosmological constants in the DGP model, the best-fit of *Brane 2* turns out to be the  $\Lambda$ CDM model while *Brane 1* can fit slightly better than that. Lastly, we also included a plot of luminosity distance of both *Brane 1* and *Brane 2* against the observed data in Figure 12. This also shows that the models are largely indistinguishable.

Model	Data Set	$\Omega_M$	$\Omega_{r_c}$	$\Omega_B$	$\Omega_\Lambda$	$\chi^2$
<i>Brane 1</i>	SNLS	0.3	0.02	-1.00	0.70	300.3916
<i>Brane 2</i>	SNLS	0.3	0	-1.00	0.70	318.3544

Table 9: Best-fit of *Brane 1* and *Brane 2* assuming a flat universe with  $\Omega_M = 0.3$ .

Model	Data Set	$\Omega_M$	$\Omega_{r_c}$	$\Omega_\Lambda$	$\chi^2$
<i>Brane 1</i>	SNLS	0.817	9.99	6.504	301.2647
<i>Brane 2</i>	SNLS	0.214	0	0.786	301.5454

Table 10: Best-fit of *Brane 1* and *Brane 2* assuming a flat universe with only the brane constant.

Model	Data Set	$\Omega_M$	$\Omega_{r_c}$	$\Omega_\Lambda$	$\chi^2$
<i>Brane 1</i>	SNLS	0.3	0.204	1.603	301.3920
<i>Brane 2</i>	SNLS	0.3	0	0.700	318.3544

Table 11: Best-fit of *Brane 1* and *Brane 2* assuming a flat universe with only the brane constant and  $\Omega_M = 0.3$ .

Model	Data Set	$\Omega_M$	$\Omega_{r_c}$	$\Omega_B$	$\chi^2$
<i>Brane 2</i>	SNLS	0.213	0.001	153.8423	301.5455

Table 12: Best-fit of *Brane 2* assuming a flat universe with only the bulk constant.

Model	Data Set	$\Omega_M$	$\Omega_{r_c}$	$\Omega_B$	$\chi^2$
<i>Brane 2</i>	SNLS	0.3	0.880	-0.861	302.9843

Table 13: Best-fit of *Brane 2* assuming a flat universe with only the bulk constant and  $\Omega_M = 0.3$ .

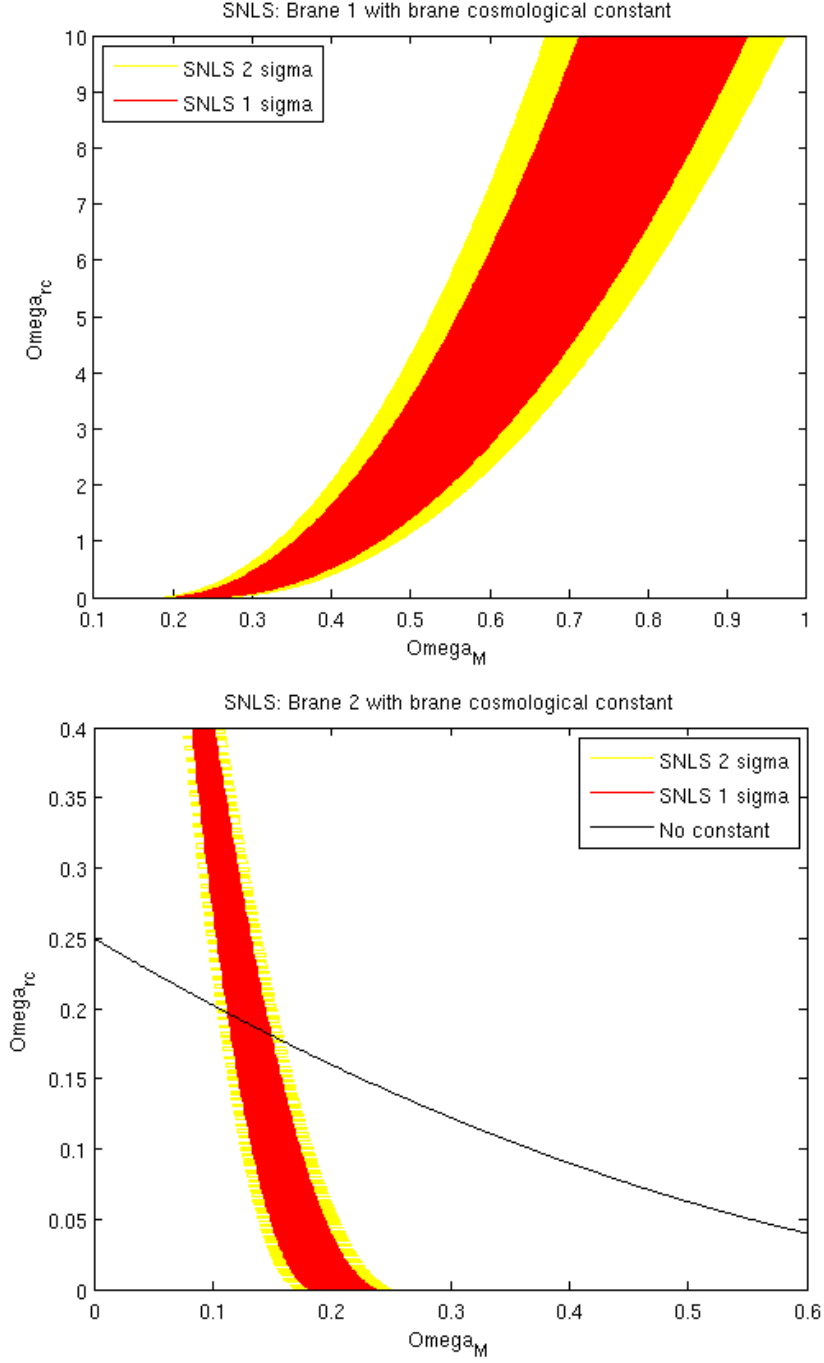


Figure 11: The fitting result of *Brane 1* and *Brane 2* with the brane constant using the SNLS data. The solid curve corresponds to the case when  $\Omega_\Lambda = 0$ .

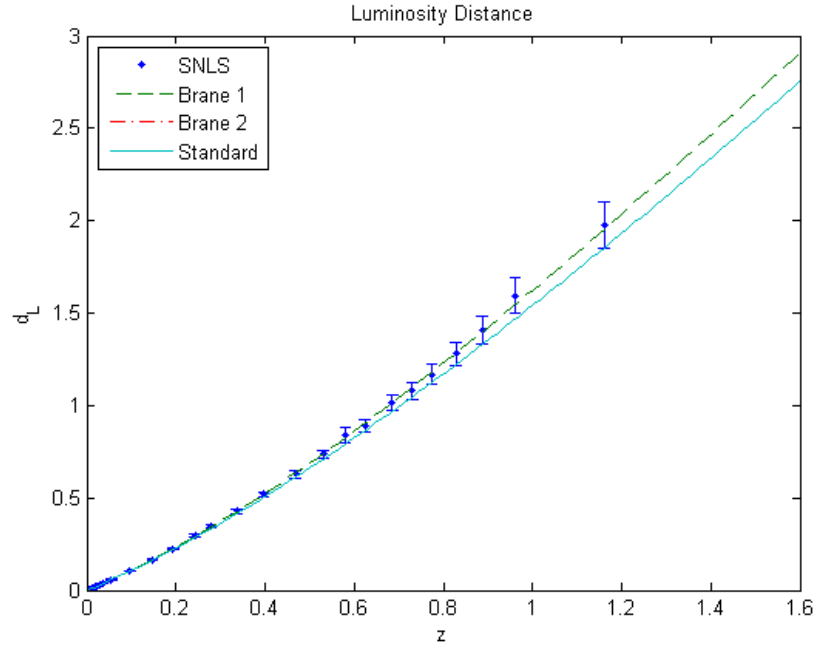


Figure 12: The plot of luminosity distance using the best-fit of Table 9. Note that *Brane 2* overlaps with  $\Lambda$ CDM (Standard) because  $\Omega_{rc} = 0$ .



## 6 Future Investigation

In the previous sections, we have seen that the DGP model has some very interesting cosmological consequences, and further examination may show that the model is a potential cosmological model. On the other hand, there are other areas of the model that worth investigating besides the cosmological solution, and there may be more to the model than self-accelerating solution. Besides exploiting other aspects of the model, there are some promising generalizations of the model proposed by the cosmologists. In this section, we present some of the work that we have briefly covered.

### 6.1 Schwarzschild Solution

Besides finding the cosmological solution, a natural step in the study of any gravity theory would be to consider a local solution. There are many different local tests or scenarios that we can put our model into, here we choose one of the more popular one which is the Schwarzschild solution. In this scenario, we try to construct a local solution which is centered about a single spherical mass with no other notable energy sources nearby. In other words, we will try to repeat the process in the previous chapters but with a different metric.

We are trying to construct a solution with 3D spherical symmetry and with all the energy focused at the center, so we propose the following metric:

$$ds^2 = -e^{N(r,y)} dt^2 + e^{A(r,y)} dr^2 + r^2(d\theta^2 + \sin^2 \theta d\phi^2) + dy^2 \quad (190)$$

This metric is much like the normal metric for Schwarzschild solution. It has a spherical symmetry in our three observable spatial dimensions as can be seen in the  $\theta$  and  $\phi$  terms. On the other hand, the exponential form of the metric ensures the positivity of the spatial coefficient while the time coordinate has an opposite sign as usual. Note that for simplicity we only consider a flat and simple 5th dimension with coefficient 1 in front of the  $y$ -coordinate.

With the proposed metric, we can proceed to calculate the Christoffel symbols like in Section 2 using Equation (33). Note that in this section, the independent variables are different compare to those in the other sections, so only in this section, we use dot to denote differentiation with respect to  $r$ , while prime denotes differentiation with respect to

y. The Christoffel symbols are then given by:

$$\begin{aligned}
\Gamma_{tt}^t &= 0 & \Gamma_{tt}^r &= \frac{1}{2}e^{N-A}\dot{N} & \Gamma_{tt}^y &= \frac{1}{2}e^N N' \\
\Gamma_{tr}^t &= \frac{1}{2}\dot{N} & \Gamma_{tr}^r &= 0 & \Gamma_{tr}^y &= 0 \\
\Gamma_{ty}^t &= \frac{1}{2}N' & \Gamma_{ty}^r &= 0 & \Gamma_{ty}^y &= 0 \\
\Gamma_{rr}^t &= 0 & \Gamma_{jk}^i &= \frac{1}{2}\gamma^{im}(\gamma_{mj,k} + \gamma_{mk,j} - \gamma_{jk,m}) & \Gamma_{rr}^y &= -\frac{1}{2}e^A A' \\
\Gamma_{ry}^t &= 0 & \Gamma_{ry}^r &= \frac{1}{2}A' & \Gamma_{ry}^y &= 0 \\
\Gamma_{yy}^t &= 0 & \Gamma_{yy}^r &= 0 & \Gamma_{yy}^y &= 0
\end{aligned} \tag{191}$$

From the Christoffel symbols, we can calculate the bulk Ricci tensor using the same formula (36) and we get:

$$\begin{aligned}
R_{tt} &= \frac{e^N}{2} \left( N'' + \frac{N'^2}{2} + \frac{N'A'}{2} \right) + e^{N-A} \left( \frac{\ddot{N}}{2} + \frac{\dot{N}^2}{4} - \frac{\dot{N}\dot{A}}{4} + \frac{\dot{N}}{r} \right) \\
R_{rr} &= \frac{e^A}{2} \left( A'' - \frac{N'A'}{2} - \frac{A'^2}{2} \right) - \frac{\ddot{N}}{2} - \frac{\dot{N}^2}{4} + \frac{\dot{N}\dot{A}}{4} + \frac{\dot{A}}{r} \\
R_{\theta\theta} &= 1 - e^{-A} - \frac{e^{-A}r^2}{2} \left( \frac{\dot{N}}{r} - \frac{\dot{A}}{r} \right) \\
R_{\phi\phi} &= \sin^2 \theta - e^{-A} \sin^2 \theta - \frac{e^{-A}r^2 \sin^2 \theta}{2} \left( \frac{\dot{N}}{r} - \frac{\dot{A}}{r} \right) \\
R_{yy} &= -\frac{N''}{2} - \frac{A''}{2} - \frac{N'^2}{4} - \frac{A'^2}{4} \\
R_{ry} &= -\frac{\dot{N}}{4}(N' - A') + \frac{A'}{r} - \frac{\dot{N}'}{2}
\end{aligned} \tag{192}$$

If we go on to find the bulk Einstein's tensor, we get:

$$\begin{aligned}
G_{tt} &= e^N \left( \frac{A''}{2} - \frac{A'^2}{4} + \frac{1}{r^2} \right) + e^{N-A} \left( \frac{\dot{A}}{r} - \frac{1}{r^2} \right) \\
G_{rr} &= e^A \left( \frac{N''}{2} + \frac{N'^2}{4} - \frac{1}{r^2} \right) + \frac{\dot{N}}{r} + \frac{1}{r^2} \\
G_{\theta\theta} &= \frac{r^2}{2} \left( N'' + A'' + \frac{N'^2}{2} + \frac{N'A'}{2} + \frac{A'^2}{2} \right) + \frac{e^{-A}r^2}{2} \left( \ddot{N} + \frac{\dot{N}^2}{2} - \frac{\dot{N}\dot{A}}{2} + \frac{\dot{N}}{r} - \frac{\dot{A}}{r} \right) \\
G_{\phi\phi} &= \frac{r^2 \sin^2 \theta}{2} \left( N'' + A'' + \frac{N'^2}{2} + \frac{N'A'}{2} + \frac{A'^2}{2} \right) + \frac{e^{-A}r^2 \sin^2 \theta}{2} \left( \ddot{N} + \frac{\dot{N}^2}{2} - \frac{\dot{N}\dot{A}}{2} + \frac{\dot{N}}{r} - \frac{\dot{A}}{r} \right) \\
G_{yy} &= \frac{N'A'}{4} - \frac{1}{r^2} + e^{-A} \left( \frac{\ddot{N}}{2} + \frac{\dot{N}^2}{4} - \frac{\dot{N}\dot{A}}{4} + \frac{\dot{N}}{r} - \frac{\dot{A}}{r} + \frac{1}{r^2} \right) \\
G_{ry} &= -\frac{\dot{N}}{4}(N' - A') + \frac{A'}{r} - \frac{\dot{N}'}{2}
\end{aligned} \tag{193}$$

Since we are considering the Schwarzschild solution, we will be solving the equations assuming an empty space, i.e.  $T_{AB} = 0$ . Hence the source part of the equation only consists of the scalar curvature term  $U$  (27). From the expression of the Einstein tensor,  $U_{AB}$  can be found simply by removing the terms involving the differentiation with respect to  $y$  and adding the leading coefficient:

$$\begin{aligned}
U_{tt} &= -\frac{\delta(y)}{\mu^2} \left[ e^{N-A} \left( \frac{\dot{A}}{r} - \frac{1}{r^2} \right) + \frac{e^N}{r^2} \right] \\
U_{rr} &= -\frac{\delta(y)}{\mu^2} \left( \frac{\dot{N}}{r} + \frac{1}{r^2} - \frac{e^A}{r^2} \right) \\
U_{\theta\theta} &= -\frac{e^{-A}r^2\delta(y)}{2\mu^2} \left( \ddot{N} + \frac{\dot{N}^2}{2} - \frac{\dot{N}\dot{A}}{2} + \frac{\dot{N}}{r} - \frac{\dot{A}}{r} \right) \\
U_{\phi\phi} &= -\frac{e^{-A}r^2 \sin^2 \theta \delta(y)}{2\mu^2} \left( \ddot{N} + \frac{\dot{N}^2}{2} - \frac{\dot{N}\dot{A}}{2} + \frac{\dot{N}}{r} - \frac{\dot{A}}{r} \right)
\end{aligned} \tag{194}$$

Then, similar to Section 3.2, we can now consider the boundary conditions in the brane. By assuming a discontinuity in  $A'$  at  $y = 0$  and hence a  $\delta(y)$  in  $A''$ , we can equate the  $\delta(y)$

terms on both sides of the equations to get:

$$\begin{aligned}
A' &= -\frac{\kappa^2}{\mu^2} \left[ e^{-A} \left( \frac{\dot{A}}{r} - \frac{1}{r^2} \right) + \frac{1}{r^2} \right] \\
N' &= -\frac{\kappa^2}{\mu^2} \left[ e^{-A} \left( \frac{\dot{N}}{r} + \frac{1}{r^2} \right) - \frac{1}{r^2} \right] \\
N' + A' &= -\frac{\kappa^2 e^{-A}}{2\mu^2} \left( \ddot{N} + \frac{\dot{N}^2}{2} - \frac{\dot{N}\dot{A}}{2} + \frac{\dot{N}}{r} - \frac{\dot{A}}{r} \right)
\end{aligned} \tag{195}$$

Note that we have also assumed a  $\mathbb{Z}^2$  symmetry and substitute  $[A'] = 2A'(0+)$  in the equation.

If we combine the equations, we get:

$$\begin{aligned}
-\frac{\kappa^2 e^{-A}}{\mu^2} \left( \frac{\dot{A}}{r} + \frac{\dot{N}}{r} \right) &= -\frac{\kappa^2 e^{-A}}{2\mu^2} \left( \ddot{N} + \frac{\dot{N}^2}{2} - \frac{\dot{N}\dot{A}}{2} + \frac{\dot{N}}{r} - \frac{\dot{A}}{r} \right) \\
\frac{e^{-A}}{2\mu^2} \left( \ddot{N} + \frac{\dot{N}^2}{2} - \frac{\dot{N}\dot{A}}{2} - \frac{\dot{N}}{r} - \frac{3\dot{A}}{r} \right) &= 0
\end{aligned} \tag{196}$$

This gives us a first simplified equation of the Einstein equations. Although we have eliminated the dependence of  $y$  in this equation, we still need at least one more equation to solve for the two variables  $N$  and  $A$ .

Similar to Section 2.7, we try to find an integral form of the Einstein equations by defining  $F(r, y)$ :

$$F(r, y) = e^N N'^2 + e^{N-A} \dot{N}^2 \tag{197}$$

Then we can calculate  $F'$  and  $\dot{F}$  and relate them to the Einstein's tensor:

$$\begin{aligned}
F' &= e^N N'^3 + 2e^N N' N'' + e^{N-A} \dot{N}^2 (N' - A') + 2e^{N-A} \dot{N} \dot{N}' \\
&= 4e^N N' \underbrace{\left( \frac{1}{2} N'' + \frac{1}{4} N'^2 \right)}_{G_{rr}} + 4e^{N-A} \dot{N} \underbrace{\left[ \frac{\dot{N}}{4} (N' - A') + \frac{\dot{N}'}{2} \right]}_{G_{ry}}
\end{aligned} \tag{198}$$

$$\begin{aligned}
\dot{F} &= e^N \dot{N} N'^2 + 2e^N N' \dot{N}' + e^{N-A} \dot{N}^2 (\dot{N} - \dot{A}) + 2e^{N-A} \dot{N} \ddot{N} \\
&= e^N N' \left( 2\dot{N}' + \dot{N} N' - \dot{N} A' \right) + e^N \dot{N} N' A' + e^{N-A} \dot{N} \left( \dot{N}^2 - \dot{N} \dot{A} + 2\ddot{N} \right) \\
&= 4e^N N' \underbrace{\left[ \frac{\dot{N}}{4} (N' - A') + \frac{\dot{N}'}{2} \right]}_{G_{ry}} + 4e^N \dot{N} \underbrace{\left[ \frac{N' A'}{4} + e^{-A} \left( \frac{\ddot{N}}{2} + \frac{\dot{N}^2}{4} - \frac{\dot{N} \dot{A}}{4} \right) \right]}_{G_{yy}}
\end{aligned} \tag{199}$$

We can see that  $F$  defined as such seems hopeful in giving us the integral form, but in the end the appropriate  $F$  proves to be too elusive and the search for a second equation independent of  $y$  turned out fruitless.

In summary, the differential equation for the Schwarzschild solution is too complicated to be solved analytically, but from the discussion in Section 3.4, we saw that the model should hold in smaller scales like the solar system, so if one was to solve the equations numerically, it shall give the same conclusion that the model doesn't deviate from the usual Schwarzschild solution for small  $r$ .

## 6.2 Schwarzschild Solution Again

After the the previous attempt has failed, we tried to find a Schwarzschild solution again by proposing a different version of the metric:

$$ds^2 = -N^2(r, y) dt^2 + A^2(r, y) dr^2 + r^2 (d\theta^2 + \sin^2 \theta d\phi^2) + dy^2 \tag{200}$$

Here we have kept the spherical symmetry of the solution in the  $\theta$  and  $\phi$  terms, but instead of using exponentials, we use square terms to ensure the positivity of the coefficients. The part involving the 5th coordinate  $y$  is still given in its simplest form.

Using the second metric proposed, we proceed to calculate the Christoffel symbols again:

$$\begin{array}{lll}
\Gamma_{tt}^t = 0 & \Gamma_{tt}^r = \frac{N\dot{N}}{A^2} & \Gamma_{tt}^y = NN' \\
\Gamma_{tr}^t = \frac{\dot{N}}{N} & \Gamma_{tr}^r = 0 & \Gamma_{tr}^y = 0 \\
\Gamma_{ty}^t = \frac{N'}{N} & \Gamma_{ty}^r = 0 & \Gamma_{ty}^y = 0 \\
\Gamma_{rr}^t = 0 & \Gamma_{jk}^i = \frac{1}{2} \gamma^{im} (\gamma_{mj,k} + \gamma_{mk,j} - \gamma_{jk,m}) & \Gamma_{rr}^y = -AA' \\
\Gamma_{ry}^t = 0 & \Gamma_{ry}^r = \frac{A'}{A} & \Gamma_{ry}^y = 0 \\
\Gamma_{yy}^t = 0 & \Gamma_{yy}^r = 0 & \Gamma_{yy}^y = 0
\end{array} \tag{201}$$

From the Christoffel symbols, we can deduce the Ricci tensor:

$$\begin{aligned}
R_{tt} &= N^2 \left( \frac{N''}{N} + \frac{N'A'}{NA} + \frac{\ddot{N}}{NA^2} - \frac{\dot{N}\dot{A}}{NA^3} + \frac{2\dot{N}}{rNA^2} \right) \\
R_{rr} &= -A^2 \left( \frac{A''}{A} + \frac{N'A'}{NA} + \frac{\ddot{N}}{NA^2} - \frac{\dot{N}\dot{A}}{NA^3} - \frac{2\dot{A}}{rA^3} \right) \\
R_{\theta\theta} &= 1 - \frac{1}{A^2} - \frac{r}{A^2} \left( \frac{\dot{N}}{N} - \frac{\dot{A}}{A} \right) \\
R_{\phi\phi} &= \sin^2 \theta - \frac{\sin^2 \theta}{A^2} - \frac{r \sin^2 \theta}{A^2} \left( \frac{\dot{N}}{N} - \frac{\dot{A}}{A} \right) \\
R_{yy} &= -\frac{N''}{N} - \frac{A''}{A} \\
R_{ry} &= \frac{2A'}{rA} + \frac{\dot{N}A'}{NA} - \frac{\dot{N}'}{N}
\end{aligned} \tag{202}$$

We then contract the Ricci tensor to get the Ricci scalar:

$$R = -\frac{2N''}{N} - \frac{2A''}{A} - \frac{2N'A'}{NA} - \frac{2\ddot{N}}{NA^2} + \frac{2\dot{N}\dot{A}}{NA^3} - \frac{4\dot{N}}{rNA^2} + \frac{4\dot{A}}{rA^3} + \frac{2}{r^2} - \frac{2}{r^2 A^2} \tag{203}$$

Finally using the expression of the Ricci tensor and Ricci scalar, we arrive at the Einstein's tensor:

$$\begin{aligned}
G_{tt} &= N^2 \left( \frac{1}{r^2} - \frac{1}{r^2 A^2} - \frac{A''}{A} + \frac{2\dot{A}}{rA^3} \right) \\
G_{rr} &= -A^2 \left( \frac{1}{r^2} - \frac{1}{r^2 A^2} - \frac{N''}{N} - \frac{2\dot{N}}{rNA^2} \right) \\
G_{\theta\theta} &= r^2 \left( \frac{N''}{N} + \frac{A''}{A} + \frac{N'A'}{NA} + \frac{\ddot{N}}{NA^2} - \frac{\dot{N}\dot{A}}{NA^3} + \frac{\dot{N}}{rNA^2} - \frac{\dot{A}}{rA^3} \right) \\
G_{\phi\phi} &= r^2 \sin^2 \theta \left( \frac{N''}{N} + \frac{A''}{A} + \frac{N'A'}{NA} + \frac{\ddot{N}}{NA^2} - \frac{\dot{N}\dot{A}}{NA^3} + \frac{\dot{N}}{rNA^2} - \frac{\dot{A}}{rA^3} \right) \\
G_{yy} &= -\frac{1}{r^2} + \frac{1}{r^2 A^2} + \frac{N'A'}{NA} + \frac{\ddot{N}}{NA^2} - \frac{\dot{N}\dot{A}}{NA^3} + \frac{2\dot{N}}{rNA^2} - \frac{2\dot{A}}{rA^3} \\
G_{ry} &= \frac{2A'}{rA} + \frac{\dot{N}A'}{NA} - \frac{\dot{N}'}{N}
\end{aligned} \tag{204}$$

On the other hand, the scalar curvature term  $U$  (27) is given by:

$$\begin{aligned}
U_{tt} &= -\frac{N^2\delta(y)}{\mu^2} \left( \frac{1}{r^2} - \frac{1}{r^2 A^2} + \frac{2\dot{A}}{r A^3} \right) \\
U_{rr} &= \frac{A^2\delta(y)}{\mu^2} \left( \frac{1}{r^2} - \frac{1}{r^2 A^2} - \frac{2\dot{N}}{r N A^2} \right) \\
U_{\theta\theta} &= -\frac{r^2\delta(y)}{\mu^2} \left( \frac{\ddot{N}}{N A^2} - \frac{\dot{N}\dot{A}}{N A^3} + \frac{\dot{N}}{r N A^2} - \frac{\dot{A}}{r A^3} \right) \\
U_{\phi\phi} &= -\frac{r^2 \sin^2 \theta \delta(y)}{\mu^2} \left( \frac{\ddot{N}}{N A^2} - \frac{\dot{N}\dot{A}}{N A^3} + \frac{\dot{N}}{r N A^2} - \frac{\dot{A}}{r A^3} \right)
\end{aligned} \tag{205}$$

The next step is again finding the junction condition. Assuming the jump in  $A'$  and the  $\delta(y)$  in  $A''$ , we equate the terms involving  $\delta(y)$  on both sides of the Einstein's equations and get:

$$\begin{aligned}
-\frac{2A'}{A} &= -\frac{\kappa^2}{\mu^2} \left( \frac{1}{r^2} - \frac{1}{r^2 A^2} + \frac{2\dot{A}}{r A^3} \right) \\
-\frac{2N'}{N} &= -\frac{\kappa^2}{\mu^2} \left( \frac{1}{r^2} - \frac{1}{r^2 A^2} - \frac{2\dot{N}}{r N A^2} \right) \\
\frac{2A'}{A} + \frac{2N'}{N} &= -\frac{\kappa^2}{\mu^2} \left( \frac{\ddot{N}}{N A^2} - \frac{\dot{N}\dot{A}}{N A^3} + \frac{\dot{N}}{r N A^2} - \frac{\dot{A}}{r A^3} \right)
\end{aligned} \tag{206}$$

If we combine the equations, we get:

$$\frac{\ddot{N}}{N A^2} - \frac{\dot{N}\dot{A}}{N A^3} - \frac{\dot{N}}{r N A^2} + \frac{\dot{A}}{r A^3} + \frac{2}{r^2} - \frac{2}{r^2 A^2} = 0 \tag{207}$$

Thus we have arrived at a nice equation involving only  $r$ -related terms, but we still need a second equation to solve for the variables  $N$  and  $A$ .

To get a second equation with only  $r$ -related terms, instead of trying to find an integral form of the Einstein equation like in the previous attempt, we return to the basic and manipulate directly the Einstein tensor. If we consider  $G_{\theta\theta}/r^2 + G_{tt}/N^2 - G_{rr}/A^2 - G_{yy}$ ,

we get:

$$-\frac{3\dot{N}}{rNA^2} + \frac{3\dot{A}}{rA^3} + \frac{3}{r^2} - \frac{3}{r^2A^2} = -\frac{\kappa^2\delta(y)}{\mu^2} \left( \frac{\ddot{N}}{NA^2} - \frac{\dot{N}\dot{A}}{NA^3} - \frac{\dot{N}}{rNA^2} + \frac{\dot{A}}{rA^3} + \frac{2}{r^2} - \frac{2}{r^2A^2} \right) \quad (208)$$

Since one side of the equation is a delta distribution while the other is not, they must both be zero. Note that on the right-hand side we have the same equation as the one coming from the junction condition. This is not surprising since the junction condition is also resulted from the manipulation of the  $\delta(y)$  terms. However, we have the second equation that we are looking for on the left-hand side:

$$-\frac{\dot{N}}{rNA^2} + \frac{\dot{A}}{rA^3} + \frac{1}{r^2} - \frac{1}{r^2A^2} = 0 \quad (209)$$

After we have found the two equations of  $N$  and  $A$  that involve only  $r$ , it seems hopeful to find solution, but after much effort, the system of differential equations proves to be beyond my reach. Unfortunately, the attempt to search for a Schwarzschild solution has failed again.

### 6.3 Diluting Cosmological Constant

From the previous discussions, we see that although the DGP model has many interesting properties, it doesn't fit the observation better than the  $\Lambda$ CDM, so there is still room for improvement. Since the publication of the DGP model in 2000 [2], many cosmologists have studied and proposed various ways of generalizing the model. There are several methods of generalization that stand out from the rest because they change the model from fundamental and hence is more promising in giving a different result from the original DGP model. These methods include the direct generalization of the DGP model with a higher dimensional bulk [7] and a step-by-step generalization into the cascading gravity models [22][23]. We include here a brief introduction to the former which is the model of diluting cosmological constant. This shows that more can be done to the higher dimensional cosmology.

In a paper [7], two of the original authors of the DGP model, Dvali and Gabadadze working with Shifman to propose a new model that involves not only 1 but more than 2 extra dimensions. In this setting, we are assumed to live in a 3D brane that is embedded in a bulk of  $(4+N)$ -dimension, where  $N$  is the number of extra dimensions and  $N > 2$ . In



this setting, the action is given by:

$$S = M_*^{2+N} \int d^4x d^N \rho \sqrt{-\tilde{g}} \tilde{R} + M_{(4)}^2 \int d^4x \sqrt{-g} R + \int d^4x \sqrt{-g} (\varepsilon + L_m) \quad (210)$$

where  $x$  is the usual 4D coordinate,  $\rho$  is the coordinate for the  $N$  extra dimensions, the tilded terms are as before the bulk quantities while the normal ones are the brane quantities,  $M_*$  is the  $(4+N)$ -dimensional Planck mass while  $M_{(4)}$  is the usual 4D equivalent. Note that in this setting, we only assume a source term that is comprised of a 4D brane cosmological constant,  $\varepsilon$  and a 4D matter lagrangian,  $L_m$ .

One of the up-side of having even more dimensions is to solve the fine-tuning problem of the cosmological constant. Put it simply, diluting the cosmological constant is needed because models like the  $\Lambda$ CDM model with a cosmological constant of natural value  $(\sim(\text{TeV})^4)$  doesn't predict the observed small value of the Hubble parameter. More precisely, by accepting that the current universe is dominated by the cosmological constant,  $H$  is given by the usual Friedmann's equation (53):

$$H^2 \sim \frac{1}{M_{Pl}^2} \varepsilon \quad (211)$$

Substituting into the equation the value of Planck mass, this gives a Hubble parameter of  $H \sim 10^{-3}\text{eV}$  which is largely inconsistent with the observed  $H \sim 10^{-33}\text{eV}$ . The only way to make the standard model work is by using a large amount of fine tuning to cancel the effect of the cosmological constant.

Thankfully in this model of diluting cosmological constant, the fine-tuning problem is avoided. The energy filter shields most of the effect of a large cosmological constant and predicts a small Hubble parameter as observed:

$$\begin{aligned} H &\sim 10^{-33}\text{eV for } N = 4, M_* \sim 10^{-3}\text{eV}, \varepsilon'_4 \sim (\text{TeV})^4 \\ H &\sim 10^{-33}\text{eV for } N = 6, M_* \sim 10^{-3}\text{eV}, \varepsilon'_4 \sim M_{Pl}^4 \end{aligned} \quad (212)$$

This solves the cosmological constant problem. As a future work to study the higher dimensional cosmology, it would be interesting to fit the diluting cosmological constant model to the observations.

## 7 Conclusion

Throughout this thesis, we have studied extensively the DGP model. From the proposed action, we have rederived the Einstein's equations and the Friedmann equation. We also showed that the braneworld models with a static brane embedded in a bulk can be constructed smoothly at the boundaries. Using the equation of motion, we found the expression for  $H$  and we saw that the model has two branches of solutions with different properties. In particular, the *Brane 1* solution resembles the phantom energy model without violating the energy conservation. This suggests an interesting idea that the phantom energy discussions are not completely impossible and that models with effective equation of state less than  $-1$  are still valid alternatives in solving the cosmological constant problem. This opens up a lot more possibilities for the cosmologist community.

We then proceed to give some comments on the cosmology of the DGP model by comparing the model to the widely accepted  $\Lambda$ CDM model. After testing the DGP model thoroughly with the minimum  $\chi^2$  test, we have come to a conclusion that although *Brane 2* has self-accelerating solutions without the cosmological constant, it does not fit the observations better than the standard  $\Lambda$ CDM model. Without a cosmological constant, *Brane 2* lacks the acceleration that we see today. When the cosmological constant is added, *Brane 2*'s best-fit turns out to be equivalent to the  $\Lambda$ CDM model. On the other hand, although being constrained by not able to produce a flat universe without the cosmological constants, *Brane 1* fits better to the supernova data than the  $\Lambda$ CDM model in a flat universe with brane and bulk cosmological constants and the best-fit matter density is not far from the value measured from other observations. When  $\Omega_M$  is constrained to 0.3, the DGP model fares as well as the standard model, until future observations can distinguish the two.

The DGP model with a cosmological constant does not solve the cosmological constant problem. As we saw in the fitting, the value of the cosmological constant has the same order as in the  $\Lambda$ CDM model, which is much smaller than the value predicted by particle physics. Our initial hope of solving the problem with the *Brane 2* self-accelerating solution is deemed unlikely when the fitting more favors the  $\Lambda$ CDM model. Although the DGP model does not fit the observations better than the commonly accepted  $\Lambda$ CDM model, it is still interesting to see that acceleration in the expansion of the universe is achievable without any dark energy.

On the other hand, the DGP model still has certain unresolved problems of its own. The extra degree of freedom for the propagator makes for a 5D massless graviton or a 4D

massive graviton, which is inconsistent with the observation [2]. The value of the cross-over scale,  $r_c$  is also questionably small due to the value of the 4D and 5D Planck masses [2]. This suggests in the DGP model there is still room for improvement and once one has proposed a generalization of the model and has solved these problems, we may be closer to solving the cosmological constant problem.

In conclusion, although the DGP model shows promising properties of having a self-accelerating *Brane 2* solution without a cosmological constant, it does not fit the observations better than the  $\Lambda$ CDM model. While the *Brane 1* solution of the DGP model shows a similar behavior to the phantom energy model and fits slightly better than the  $\Lambda$ CDM model, the cosmological constant is still needed in the model and its value is at the same order as that in the  $\Lambda$ CDM model. To solve the problem, we have to try to generalize the DGP model. One of the more promising generalizations is discussed in Section 6.3. Future work on this model of diluting cosmological constant may reveal a better solution to the cosmological constant problem.

## Annex: Matlab Code

```
% Brane 1 with brane and bulk cosmological constant
clear;
load SNLS_data;

a = 1.451;
b = 3.165;
chi2min = 500;
chi2mat = zeros(101,201) + 5000;
for Omega_lambda = 0.7:0.01:1.7
    for Omega_B = -1:0.01:1
        X2 = 0;
        C1 = 0;
        C2 = 0;
        if Omega_lambda == 0.7 && Omega_B == -1
            % degenerated case
            chi2temp = 5000;
            for Omega_r_c = 0:0.01:1
                X2 = 0;
                C1 = 0;
                C2 = 0;
                for i = 1:size(SNLS,1)
                    d_L =
                        luminosityDBrane1Brane5DConst_degen(SNLS(i,1), Omega_r_c);
                    if d_L == 0
                        % The (Omega_lambda, Omega_B) pair is inadmissible
                        X2 = 5000;
                        C1 = 0;
                        C2 = 1;
                        break;
                    else
                        m_mod = 5*log(d_L)/log(10) + 42.384 - a*(SNLS(i,3)-1)
                            + b*SNLS(i,4);
                        X2 = X2 + (m_mod - SNLS(i,2))^2/SNLS(i,5);
                        C1 = C1 + (m_mod - SNLS(i,2))/SNLS(i,5);
                    end
                end
            end
        end
    end
end
```

```

        C2 = C2 + 1/SNLS(i,5);
    end
end
chi2 = X2 - C1^2/C2 + log(C2/(2*pi));
if chi2 < chi2temp
    chi2temp = chi2;
    orc_degen = Omega_r_c;
end
end
chi2mat(1,1) = chi2temp;
if chi2temp < chi2min
    chi2min = chi2temp;
    ob_best = -1;
    ol_best = 0.7;
end
else
    for i = 1:size(SNLS,1)
        d_L =
            luminosityDBrane1Brane5DConst(SNLS(i,1), Omega_lambda, Omega_B);
        if d_L == 0
            X2 = 5000; %The (Omega_lambda, Omega_B) pair is inadmissible
            C1 = 0;
            C2 = 1;
            break;
        else
            m_mod = 5*log(d_L)/log(10) + 42.384 - a*(SNLS(i,3)-1)
                + b*SNLS(i,4);
            X2 = X2 + (m_mod - SNLS(i,2))^2/SNLS(i,5);
            C1 = C1 + (m_mod - SNLS(i,2))/SNLS(i,5);
            C2 = C2 + 1/SNLS(i,5);
        end
    end
end
chi2 = X2 - C1^2/C2 + log(C2/(2*pi));
l_i = cast(100*(Omega_lambda-0.7) + 1, 'int16');
B_i = cast(100*(Omega_B+1) + 1, 'int16');
chi2mat(l_i,B_i) = chi2;

```

```
        if chi2 < chi2min
            chi2min = chi2;
            ob_best = Omega_B;
            ol_best = Omega_lambda;
        end
    end
end
end

save analytic_chi_square_test_result orc_degen ol_best ob_best chi2min chi2mat;
```

```

function [d_L] = luminosityDBrane1Brane5DConst_degen(z, Omega_r_c)
%   Luminosity distance (dimensionless) d_L*H_0/c
%   flat with brane and bulk constant, Omega_M = 0.3
Omega_lambda = 0.7;
Omega_B = -1;

function [E] = E(z)
%   Reduced Hubble parameter, E = H/H_0
E = sqrt(0.3*(1+z).^3 + Omega_lambda + 2*Omega_r_c
        - 2*sqrt(Omega_r_c)
        *sqrt(Omega_lambda+Omega_r_c+Omega_B+0.3*(1+z).^3));
end

function [EInv] = EInv(z)
%   Inverse of E
EInv = 1./E(z);
end

function [d_C] = d_C(z)
d_C = integral(@EInv,0,z);
end

function [d_M] = comovingD(z)
%   Comoving distance
d_M = d_C(z);
end

d_L_temp = (1+z)*comovingD(z);
if isreal(d_L_temp)
    d_L = abs(d_L_temp);
else
    d_L = 0;
end
end

```

```

function [d_L] = luminosityDBrane1Brane5DConst(z, Omega_lambda, Omega_B)
%   Luminosity distance (dimensionless) d_L*H_0/c
%   flat with brane and bulk constant, Omega_M = 0.3

Omega_r_c = (Omega_lambda-0.7)^2/(4*(1+Omega_B));

function [E] = E(z)
%   Reduced Hubble parameter, E = H/H_0
E = sqrt(0.3*(1+z).^3 + Omega_lambda + 2*Omega_r_c
        - 2*sqrt(Omega_r_c)
        *sqrt(Omega_lambda+Omega_r_c+Omega_B+0.3*(1+z).^3));
end

function [EInv] = EInv(z)
%   Inverse of E
EInv = 1./E(z);
end

function [d_C] = d_C(z)
d_C = integral(@EInv,0,z);
end

function [d_M] = comovingD(z)
%   Comoving distance
d_M = d_C(z);
end

d_L_temp = (1+z)*comovingD(z);
if isreal(d_L_temp)
    d_L = abs(d_L_temp);
else
    d_L = 0;
end
end

```



## References

- [1] E. J. Copeland, M. Sami and S. Tsujikawa, Int. J. Mod. Phys. D 15:1753-1936 (2006) [hep-th/0603057v3]
- [2] G. Dvali, G. Gabadadze and M. Porrati, Phys. Lett. B 485:208-214 (2000) [hep-th/0005016v2]
- [3] P. S. Wesson, *Space-Time-Matter: Modern Higher-Dimensional Cosmology*, 2nd Edition, 2007, World Scientific Publishing Co., Pte. Ltd., ISBN-10 981-270-632-1; ISBN-13 978-981-270-632-4.
- [4] L. Randall and R. Sundrum, Phys. Rev. Lett. 83:3370-3373 (1999) [hep-ph/9905221]
- [5] C. Deffayet, Phys. Lett. B 502:199-208 (2001) [hep-th/0010186v2]
- [6] V. Sahni and Y. Shtanov, JCAP 0311 014 (2003) [astro-ph/0202346v3]
- [7] G. Dvali, G. Gabadadze and M. Shifman, Phys. Rev. D 67:044020 (2003) [hep-th/0202174v2]
- [8] P. Binetruy, C. Deffayet, U. Ellwanger and D. Langlois, Phys. Lett. B 477:285-291 (2000) [hep-th/9910219v2]
- [9] P. Binetruy, C. Deffayet and D. Langlois, Nucl. Phys. B 565:269-287 (2000) [hep-th/9905012v2]
- [10] Y. V. Shtanov (2000) [hep-th/0005193v3]
- [11] A. Lue and G. D. Starkman, Phys. Rev. D 70:101501 (2004) [astro-ph/0408246v2]
- [12] C. Deffayet, G. Dvali and G. Gabadadze, Phys. Rev. D 65:044023 (2002) [hep-ph/0105068v1]
- [13] W. H. Press, S. A. Teukolsky, W. T. Vetterling and B. P. Flannery, *Numerical Recipes in Fortran 77. The Art of Scientific Computing*, 2nd Edition, 1992, Cambridge University Press, ISBN 0-521-43064-X.
- [14] Y. Wang *et al.*, JCAP 12 003 (2004) [doi:10.1088/1475-7516/2004/12/003]
- [15] A. G. Riess *et al.*, Astrophys. J. 607:665-687 (2004) [astro-ph/0402512v2]
- [16] Z. Guo, Z. Zhu, J. S. Alcaniz and Y. Zhang, ApJ 646:1-7 (2006) [astro-ph/0603632v2]

- [17] M. Fairbairn and A. Goobar, Phys. Lett. B 642:432-435 (2006) [astro-ph/0511029v2]
- [18] D. J. Eisenstein *et al.*, Astrophys. J. 633:560-574 (2005) [astro-ph/0501171v1]
- [19] M. Sullivan *et al.*, ApJ. 737:102 (2011) [astro-ph/1104.1444v2]
- [20] A. Conley *et al.*, ApJS 192 1 (2011) [doi:10.1088/0067-0049/192/1/1]
- [21] U. Alam and V. Sahni [astro-ph/0209443v1]
- [22] C. de Rham, S. Hofmann, J. Khoury and A. J. Tolley, JCAP 02 011 (2003) [doi:10.1088/1475-7516/2008/02/011]
- [23] N. Agarwal, R. Bean, J. Khoury and M. Trodden, Phys. Rev. D 81:084020 (2010) [doi:10.1103/PhysRevD.81.084020]